

ECONOMIC LOSS MODELLING OF EARTHQUAKE DAMAGED BUILDINGS

Prof Michael C. Griffith^{1,2} and Dr Wade D. Lucas¹

¹The University of Adelaide

²Bushfire and Natural Hazards CRC





Version	Release history	Date
1.0	Initial release of document	22/02/2016



Australian Government
**Department of Industry,
 Innovation and Science**

Business
 Cooperative Research
 Centres Programme

This work is licensed under a Creative Commons Attribution-Non Commercial 4.0 International Licence.



Disclaimer:

The University of Adelaide and the Bushfire and Natural Hazards CRC advise that the information contained in this publication comprises general statements based on scientific research. The reader is advised and needs to be aware that such information may be incomplete or unable to be used in any specific situation. No reliance or actions must therefore be made on that information without seeking prior expert professional, scientific and technical advice. To the extent permitted by law, The University of Adelaide and the Bushfire and Natural Hazards CRC (including its employees and consultants) exclude all liability to any person for any consequences, including but not limited to all losses, damages, costs, expenses and any other compensation, arising directly or indirectly from using this publication (in part or in whole) and any information or material contained in it.

Publisher:

Bushfire and Natural Hazards CRC

February 2016

Citation: Griffith M, Lucas W (2016) Economic Loss Modelling of Earthquake Damaged Buildings, Bushfire and Natural Hazards CRC.

Cover: The Arts Centre restoration and seismic retrofit project in Christchurch, New Zealand.

Photo by Michael C. Griffith



TABLE OF CONTENTS

ABSTRACT	3
1. INTRODUCTION	4
2. DEFINITION OF HAZARD INTENSITY	8
2.1 Ground motion modelling and the associated uncertainties	8
2.2 Modelling of site effects and the associated uncertainties	11
2.3 Selection of ground motion intensity measure	12
3. CLASSIFICATION OF BUILDINGS	17
4. DEFINITION OF DAMAGE LEVELS	22
5. RELATIONSHIP BETWEEN HAZARD AND THE RESULTING BUILDING DAMAGE	29
5.1 Empirical Methods	29
5.2 Analytical vulnerability functions	35
6. CONSTRUCTION OF FRAGILITY CURVES	45
7. CONSTRUCTION OF VULNERABILITY CURVES	49
8. SUMMARY	51
REFERENCES	53



ABSTRACT

Earthquake action has only been considered in structural design in Australia since the early 1990s. With a very low building replacement rate many Australian buildings are vulnerable to major earthquakes and pose significant risk to lives, properties and economic activities. The vulnerability of buildings was evident in the Newcastle Earthquake of 1989 which has been reported to have caused damage to more than 70,000 properties and an estimated total economic loss of AU\$ 4 billion.

Models that are capable of predicting potential economic loss in future earthquakes are fundamental in the formulation of risk mitigation and retrofitting strategies. This report presents a review of the existing techniques and methodologies that have been developed for the earthquake damage loss modelling of buildings. Key components of the methodologies including definition of hazard intensity, classification of building data (developed separately by GA), definition of building damage states and definition of the relationship between the hazard intensity and resulting building damage will be discussed.

By developing an improved regional benefit-cost analysis methodology that analyses varying levels of retrofit by means of fragility curve-generated damage state probabilities, it is possible to demonstrate that the broad-scale economic benefits to the community outweigh the initial cost of a regional retrofit program. The improved methodology considers the direct economic losses, indirect regional losses to undamaged buildings, social losses due to casualties, as well as the fiscal benefits of preserving the heritage of the community. It is anticipated that this model and information that it provides will be fed to the 'Decision Support' research team.

Keywords: damage loss modelling, vulnerability assessment, economic loss, earthquakes, building



1. INTRODUCTION

The consequences of earthquakes are often catastrophic, with the collapse of structural elements posing a great risk to human life (Bertero, 1992, O'Rourke, 1996). Unreinforced masonry construction is notorious for poor performance in the case of a seismic event (Bruneau, 1994, ElGawady et al., 2004), especially in comparison with other common construction materials, such as concrete and steel. However, the majority of construction in Australia before the 1950s has historically been unreinforced masonry (URM), a large proportion of which is still occupied and hence poses significant issues for public safety in the case of an earthquake.

In seismically active areas retrofitting buildings as a precaution against earthquakes is a routine procedure and is implemented through local jurisdiction and national building codes. However, in areas of lower earthquake hazard URM structures are generally not considered to pose a potential risk and there exists little legislation mandating compulsory retrofitting of URM structures in order to mitigate possible damage. In recent history there have been devastating examples of the need to retrofit URM buildings, in particular the 2010-2011 Christchurch earthquake sequence, which resulted in the deaths of 185 people (New Zealand Police, 2012). Of the 42 deaths caused by failure of individual buildings, 39 were due to the collapse of URM façade or walls (Canterbury Earthquakes Royal Commission, 2012a). Similarly, in 1989 the usually seismically inactive city of Newcastle was hit by an earthquake of magnitude 5.6 (National Geophysical Data Centre, 2001), resulting in 13 deaths. The relatively short time period of recorded seismic data in Australia and the difficulty in accurately predicting the occurrence of earthquakes means that the estimated hazard factors within Australia may not reflect the true level of risk posed to existing URM building stock. Recent investigations by Schäfer (2014a) show that the seismic hazard levels for Adelaide in particular may be significantly underestimated. For this reason it is crucial to investigate the hypothetical financial impact of an earthquake and the effectiveness of retrofit techniques in reducing predicted losses.

In order to accurately assess the economic benefit of the systematic implementation of a regional retrofit program, various retrofit scenarios must be compared with the losses incurred if no action was taken. In some cases it may prove to be more cost effective to demolish the original structure and construct a new building entirely (Goodwin et al., 2009). There exists an extensive body of literature on URM retrofit methods, including the use of mesh-mortar surface treatments and shotcrete (ElGawady et al., 2006; Ashraf et al., 2011; Papanicolaou et al., 2011), FRP strips (Ehsani et al., 1999; Albert et al., 2001; Bruneau, 1994), post-tensioning (Fardis, 1992), epoxy injection (ElGawady et al., 2004), or even base isolation (Yao et al., 2014) or alteration of the internal load-bearing frame (Roy et al., 2013). Furthermore, when considering the options of repair versus demolition and rebuilding, the decision is again predominantly based on insured dollar value figures and there is rarely consideration for the loss of cultural identity and heritage or the collapse of a community in affected regions (Harkness, 2002).



A large percentage of the building stock built in Australia before 1935 was URM (Griffith, 2011a), with a large proportion of the buildings still being used today. Such structures possess heritage value and are a useful way of defining identity, as well as serving as a cultural record (Goodwin et al., 2009). Structural modifications to these buildings should adhere to regulations and have minimal aesthetic impact. However, there is little data on the cost of retrofit using techniques that preserve the original aesthetic of the building and the reduction in damage that they provide.

Benefit-cost analyses are a crucial step in the systematic implementation of legislative change for countries with few or no seismic hazard mitigation methods, but so far very little specific research comparing the benefits of various levels of retrofit on a broad scale has been undertaken. The lack of hard financial data and common public misconceptions surrounding seismic retrofit methods are significant deterrents in the justification of compulsory URM strengthening, as both homeowners and government departments are unable to quantify potential financial savings or loss reductions, both for physical property damages and for human life (Egbelakin, 2011). Unfortunately, public support for improvements to seismic mitigation techniques are always at highest levels during the period immediately after an earthquake event, by which time the damage has already been wrought (Nigg, 1984).

The benchmark for the retrofit of pre-existing constructions is requiring that a building be strengthened to a minimum percentage of the limit demanded by the new building standard (also referred to as percentage of new building standard, or % NBS) (Egbelakin, 2011; Bech et al., 2014). Most recently, as a result of the Royal Commission Inquiry into the Canterbury earthquakes, it was recommended that strengthening to 67 % NBS was the minimum amount that had a real benefit on reducing building damage (and therefore fatalities) (Griffith, 2011b). A benefit-cost analysis of URM retrofit levels, as ranked by predicted damage states and described in terms of % NBS, would provide invaluable insights into the feasibility of retrofit methods for specific building typologies and persuade policy-makers to improve seismic mitigation strategies.

Hazard loss estimation systems, such as PAGER, are primarily used to rapidly predict losses in the wake of a natural hazard and tend to focus on specific physical damage of buildings in dollar terms, in order to plan for disaster response and to allocate relevant aid resources (Kircher et al., 2006, Wald, 2010). However, the social and economic disruption that occurs after a natural disaster is rarely quantified, with the costs at a community level often being greater than the summation of individual building values (Stevenson, 2011, Parker and Steenkamp, 2012). The current state-of-the-art for both direct and indirect loss prediction is the US-based software package HAZUS, which requires complex data inputs that are difficult to implement in an international context. HAZUS presents a sophisticated framework for loss analysis, which provides a good basis for an Australian-based seismic loss estimation methodology.

Earthquake damage loss modelling has gained popularity driven by experiences from past events (for example, the Northridge and Kobe earthquakes which have caused an estimated economic loss of \$44 billion and \$100 billion, respectively) and the needs of end users such as emergency planners, government bodies and insurance industry. A large number of methods have



been developed for estimation of earthquake losses (e.g. Blume et al., 1977; Insurance Services Office, 1983; ATC, 1985; ATC, 1997; National Research Council, 1999). More recently, Global Earthquake Model (GEM) has been created to provide tools and resources for assessment of earthquake risk worldwide. Methodologies based on analytical and empirical vulnerability assessment have been developed for use within the GEM framework (D'Ayala et al., 2014; Rosetto et al., 2014).

Earthquake damage loss estimation software tools have been developed, with HAZUS multi-hazard software (HAZUS-MH) (FEMA, 2012) being the most notable example. Other earthquake loss estimation software tools have been developed for other regions around the world, for example, SEismic Loss EstimatioN using a logic tree Approach (SELENA) (Molina and Lindholm, 2005; Molina et al., 2010) and Displacement-Based Earthquake Loss Assessment (DBELA) (Crowley et al., 2004) for Europe, KOERILoss, AUTHLoss, and LNECLoss, for Istanbul, Lisbon, and Thessaloniki respectively, which are parts of the LESSLoss project (Spence, 2007), Geoscience Australia's Earthquake Risk Model (EQRM) for Australia (Robinson et al., 2006), and OpenQuake which is a part of GEM (Crowley et al., 2013).

Earthquake damage loss modelling requires the following aspects to be defined:

1. Intensity of hazard
2. Classification of building data
3. Levels of damage state
4. Relationship between hazard and the resulting building damage

The relationship between hazard and the resulting building damage can be defined by fragility or vulnerability functions. Fragility functions translate values of ground motion intensity measures into values of some damage measures (e.g., displacement, acceleration, inter-storey drifts). Vulnerability functions translate the ground motion intensity measures directly into values of the decision variables (e.g., monetary loss, number of buildings subjected to certain level of damage). Numerous assessment techniques have been proposed over the past decades. The assessment techniques can be broadly divided into two categories: empirical methods which are based on observation of damages and analytical methods which rely on assessing structural performance through analytical procedures.

This report presents an overview of existing methodologies and research on earthquake damage loss modelling in the context of the four aspects defined above. Section 2 discusses the definition of intensity of hazard and uncertainties associated with ground motion modelling and site effects. Section 3 describes how the classification of buildings is defined. Section 4 discusses how the damage state is commonly defined in the earthquake damage loss estimation. Section 5 presents existing research on the vulnerability assessment to develop fragility and vulnerability functions. The focus of this report is on earthquake damage loss estimations based on analytical vulnerability assessment. The important factors associated with the analytical assessment are discussed in Section 5. Sections 6 and 7 present methods and equations to construct fragility and vulnerability curves.



In this report the following research has been undertaken:

1. Establishment of a general framework to assess the direct economic losses caused by an earthquake within Australia, including the categorisation of URM building typologies in the Adelaide CBD;
2. Appraisal of heritage-listed URM buildings as providing a fiscal benefit to communities and acting as a influencing factor in favour of regional seismic retrofit;
3. Seismic retrofit design and cost estimation for one and two storey URM buildings and comparing the findings with established costs in literature;
4. Assessment of the economic feasibility of a regional seismic retrofit program in Adelaide based upon comprehensive benefit-cost analysis.



2. DEFINITION OF HAZARD INTENSITY

2.1 GROUND MOTION MODELLING AND THE ASSOCIATED UNCERTAINTIES

Ground motions in the earthquake damage loss modelling are generally defined using:

1. Deterministic analysis: ground motions corresponding to a single earthquake scenario are considered in the damage loss modelling. Ground motion demands are estimated based on the fault type, location and event magnitude chosen by the user or can be provided by the user in the form of maps of ground shaking (i.e., maps of PGA, PGV and spectral response).
 - a. “arbitrary earthquake scenario”, the user the hazard by selecting an attenuation function, earthquake scenarios and soils data.
 - b. “user supplied hazard” using ground motion maps
2. Probabilistic analysis: ground motions aggregated over a number of earthquake scenarios are considered in the damage loss modelling.

The definition of ground motion component of the earthquake damage loss estimation is a vital component as it contributes most to the overall uncertainty in the damage loss estimation (Crowley et al., 2004). There are two types of uncertainties associated with ground motion predictions (Toro et al., 1997): i) epistemic uncertainty, which is the uncertainty resulting from incomplete knowledge of the earthquake process and can therefore be reduced by acquiring additional and better data; and ii) aleatory uncertainty, which is an inherent variability and cannot be reduced without changing the predictive model.

The treatment of uncertainties in the input parameters defining the seismic demand (ground motion modelling) and seismic capacity (structural resistance) is a major component of earthquake damage loss modelling. Crowley et al. (2005) performed sensitivity analysis investigating the impact of epistemic uncertainties in the ground motion and structural resistance on the earthquake damage loss estimation. Although, the epistemic uncertainties associated with seismic resistance of the exposed building stock was found to have a large impact on the loss estimation than those associated with the seismic demand, it was also found that the epistemic uncertainties of associated with ground motion modelling has the largest influence of all the demand parameters on the loss estimation. Patchett et al. (2005) investigated the effects of aleatory and epistemic uncertainties on earthquake loss estimations. Only epistemic uncertainties associated with ground motion modelling were considered in the study. The study found that epistemic uncertainties with ground motion modelling have significant impact on the observed loss as illustrated in Figure 1. The results also indicated that epistemic uncertainties have the greatest influence of all the uncertainties considered in the study. It was suggested that multiple ground motion prediction models should be incorporated particularly if it is not clear which model is the most appropriate to a particular area.

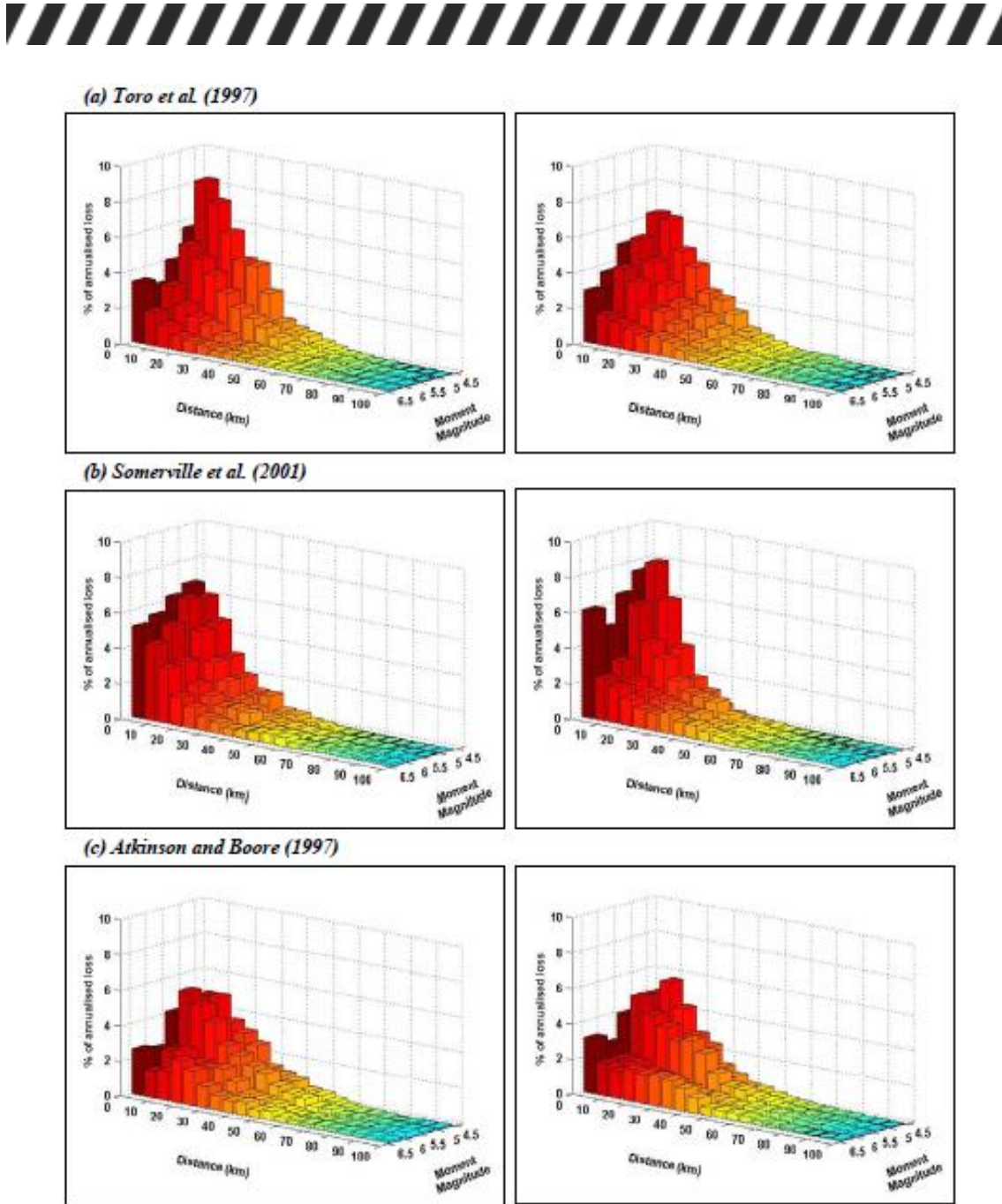


FIGURE 1 DISAGGREGATED ANNUALISED LOSS ESTIMATES IN NEWCASTLE BASED ON DIFFERENT GROUND MOTION PREDICTION MODELS (PATCHETT ET AL., 2005)

The epistemic uncertainties in the ground motion modelling are generally handled by using a range of models with different probability density functions and employing the use of logic trees. The logic trees methodology can be employed for both deterministic and probabilistic approaches to hazard analysis (Bommer et al., 2005) and has been adopted in the earthquake damage loss calculations SELINA (Molina et al., 2010) as illustrated in Figure 2. However, the use of logic trees methodology produces mean hazard values which have not been viewed as the most meaningful measure (Abrahamson and Bommer, 2004; McGuire et al., 2005; Musson, 2005).

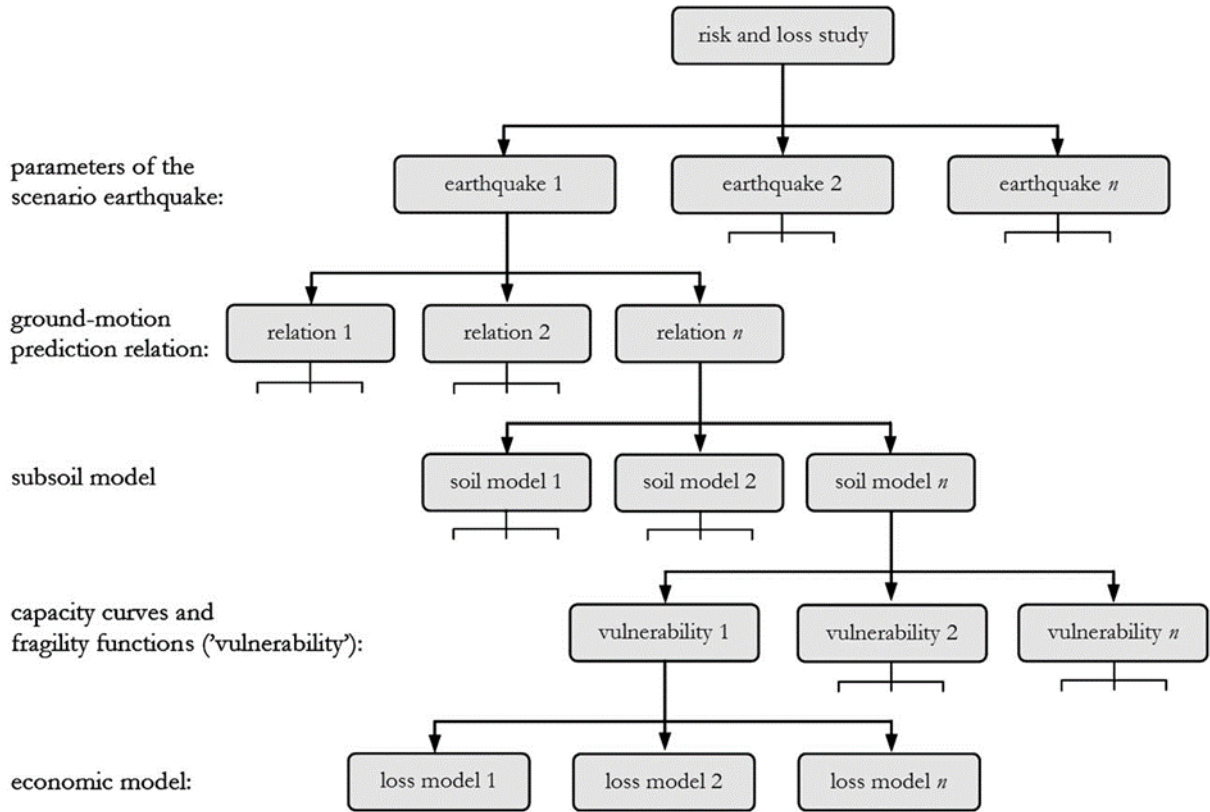


FIGURE 2 PRINCIPLE OF THE LOGIC TREE STRUCTURE IN SELENA (MOLINA ET AL., 2010)

The aleatory (random) uncertainties consist of two components of variability (Abrahamson and Youngs, 1992): inter-event variability (earthquake-to-earthquake) and intra-event variability (location-to-location). The total aleatory uncertainties σ_{total} can be taken as the square-root of the sum of the squares of the inter-event (σ_{inter}) and intra-event (σ_{intra}) as defined by Eq. (1) (Crowley et al., 2005).

$$\sigma_{total} = \sqrt{\sigma_{inter}^2 + \sigma_{intra}^2} \quad (1)$$

There are not a lot of scopes in reducing aleatory uncertainties in the ground motion modelling and hence it is important to establish an appropriate treatment for these uncertainties in the earthquake loss modelling.

Different treatments of aleatory uncertainties in both deterministic and probabilistic ground motion modelling have been discussed in detail by Bommer and Crowley (2006) and applied in a case study by Crowley and Bommer (2006). The different treatments are outlined as follows (as summarised from Bommer and Crowley, 2006):

1. When losses are calculated from single earthquake scenarios (deterministic analysis), the aleatory uncertainties are generally combined with the uncertainties in the capacity curves and incorporated into the logarithmic standard deviation of vulnerability curves in existing earthquake damage loss modelling methodologies (e.g., FEMA (2012); D'Ayala et al. (2014)). Default values of σ (referred as β in the earthquake damage loss modelling methodologies) have been recommended and they are discussed in Section 6.



2. Probabilistic seismic hazard analysis (PSHA) is a straight forward option for dealing with uncertainties when losses due to multiple earthquakes are to be calculated for a site. Hazard curves obtained from PSHA are convolved with the exposure and vulnerability of the building stock to obtain earthquake losses at each site. The main issue with using conventional PSHA for earthquake loss modelling is that the variability in ground motion that is highly spatial is completely assumed to be entirely temporal. This has been found to cause an overestimation of seismic demands (Bommer and Crowley, 2006)
3. The use of disaggregated scenarios from PSHA in earthquake loss modelling is an alternative to conducting the loss modelling directly based on PSHA results. Disaggregation of PSHA results is a process which allows the identification of individual earthquake scenarios contributing to the hazard at a selected annual frequency of exceedance. Each earthquake scenario would be used to produce demand spectra that will be convolved with the vulnerability. The loss obtained for each scenario would then need to be multiplied by the contribution of that scenario into the hazard and the losses from all scenarios would then be integrated. A major drawback of this method is that it is very computationally expensive.
4. Modification of historical earthquake catalogues. Historical catalogue alone cannot generally be used to produce vulnerability curves as it is unlikely to describe all possible events in time and space that could occur in a certain region. The historical catalogue can be supplemented by scenarios to eliminate spatial and temporal incompleteness (Bommer et al., 2002).
5. Stochastic earthquake catalogues using Monte-Carlo simulation method. The Monte-Carlo simulation method is used to generate stochastic earthquake catalogues that are temporally and spatially complete.

2.2 MODELLING OF SITE EFFECTS AND THE ASSOCIATED UNCERTAINTIES

Another key issue associated with ground motion modelling is how to account for site response. The development of GIS enables spatially distributed data, such as details of near soil conditions, to be stored efficiently. To generate a continuous spatial distribution of site conditions, interpolations between points are required as characterisation of site response is normally a point estimate.

Another source of uncertainties is the way site conditions are characterised in the earthquake loss modelling. The site conditions can be characterised in several ways (Stafford et al., 2007):

1. Geological class, based on the surface lithology
2. Geotechnical class, based on types of material and/or engineering parameters (e.g., $V_{s,30}$, SPT blow count)
3. Typical soil profile, generally based on borehole observations

Site characterisation based on borehole observations provides the best representation of site response. However, except for very well documented



cases, there is usually insufficient information to define soil profiles for the whole study area, and hence this option is rarely used in practice. Site response has often been characterised using single predictor, with average shear wave velocity over the upper 30 m ($V_{s,30}$) as the most common parameter adopted (e.g., Wills and Clahan, 2006; Kalkan et al., 2010).

The site response is affected significantly by the shear wave velocity and depth to the underlying bedrock, there are uncertainties associated with characterising soil response using average shear wave velocity for the upper 30 m layer. Nevertheless $V_{s,30}$ is often used to characterise site response in the earthquake loss estimation package (e.g., HAZUS-MH (FEMA, 2012); KOERILoss (KOERI2002, 2002); SELINA (Molina et al., 2010)). In the absence of geotechnical information, geological class is commonly used to provide site classification, a general amplification factors adopted from the code spectra or ground motion prediction equations are commonly applied in this case.

The following approaches are commonly adopted in the earthquake loss modelling packages to model the modification of the bedrock ground motion to incorporate site effects (Stafford et al., 2007):

1. Calculation of the full transfer function.
2. Modification of bedrock ground motion by frequency dependent factors
3. Modification of bedrock ground motion by frequency independent factors

Calculation of the full transfer function is rarely used in the earthquake damage loss modelling packages due to lack of information. Although a few earthquake damage loss modelling packages have this modelling approach as an option (e.g., KOERILoss (KOERI2002, 2002), LNECLoss (Campos Costa et al., 2010)). Modification through frequency dependent factors is commonly adopted in earthquake damage loss modelling packages (e.g., HAZUS-MH (FEMA, 2012); SELINA (Molina et al., 2010)). EQRM (Geoscience Australia's Earthquake Risk Model) for Australia (Robinson et al., 2006) allows for user-input amplification factors. Frequency independent factors are normally used when the ground motion is not represented by parameter that is not a reflection of its frequency content (e.g. PGA, intensity).

Effects of soil sediments on site response have been extensively investigated and issues associated with frequency-dependent factors adopted by code spectra (e.g., SA, 2007, IBC, 2006, EC8, 2004) have been highlighted in published literature (e.g., Chandler et al., 2002). There are uncertainties associated with using both frequency-dependent and independent factors in the earthquake loss modelling.

2.3 SELECTION OF GROUND MOTION INTENSITY MEASURE

Selection of ground motion intensity measure is an important factor in the earthquake damage loss modelling. Ground motion intensity can be a source of uncertainties in the damage modelling if it is not selected to depict the frequency content of ground motions which affect the structural response.

Macroseismic intensity has traditionally been adopted as the intensity parameter at which damages are being measured due to the wide availability of damage data presented in this format. For example, Braga et al. (1982) used the Medvedev–Sponheuer–Karnik (MSK) scale as intensity measures. Decanini et al. (2004) and Di Pasquale et al. (2005) used the MCS (Mercalli Cancani-Sieberg) scale due to the fact that the Italian seismic catalogue is mainly based on the MCS intensity. Studies on the correlation of loss and Gross Domestic Product have also been undertaken based on intensity based measures (e.g., Chan et al., 1998; Yong et al., 2005; Chen et al., 2005). One of the arguments for its use is that it correlates strongly with damage. However, there are three issues associated with the use of macroseismic intensity as a measure (Spence and Foulser-Piggott, 2013). Firstly, macroseismic intensity has a discrete form. As a result vulnerability relationships based on macroseismic intensity such as damage probability matrix (e.g., Whittman et al. (1973); Braga et al. (1982); Di Pasquale et al. (2005)) has a discrete form. Secondly, there are different macroseismic intensity scales used in earthquake damage loss modelling and the vulnerabilities defined in one scale are not necessarily translated to the others. Most importantly, macroseismic intensity scales are derived primarily from observations of damage. Hence, the probability of damage resulting from the earthquake loss modelling is not totally independent of the measure of ground intensity.

Continuous fragility functions and vulnerability functions that can be used to translate predicted, or observed, ground motions to damage are needed. Spence et al. (1992) introduced the Parameterless Scale Intensity (PSI) which allows continuous vulnerability functions to be derived for various types of buildings. The study also attempted to correlate the PSI to peak ground acceleration (PGA) using ground motion acceleration recorded in the vicinity of the damage survey. Sabetta et al. (1998) used post earthquake surveys to derive vulnerability functions based on ground motion parameters PGA, Effective Peak Acceleration (EPA which is defined as the maximum acceleration between natural period of 0.1 to 0.5 s) and Arias Intensity (AI which is defined as the integral of the square of the acceleration time history). An attenuation relationship developed by Sabetta and Pugliese (1996) was adopted to determine the ground motion parameters. PGA has also been adopted as a basis of vulnerable functions by more recent studies (e.g., Rota et al., 2006).

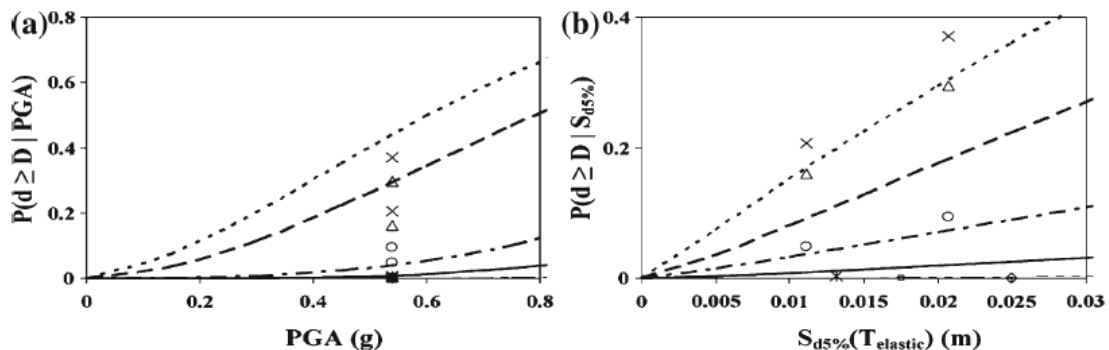


FIGURE 3 VULNERABILITY FUNCTIONS BASED ON PGA AND SD(TELASTIC) (ROSSETTO AND ELNASHAI, 2003)

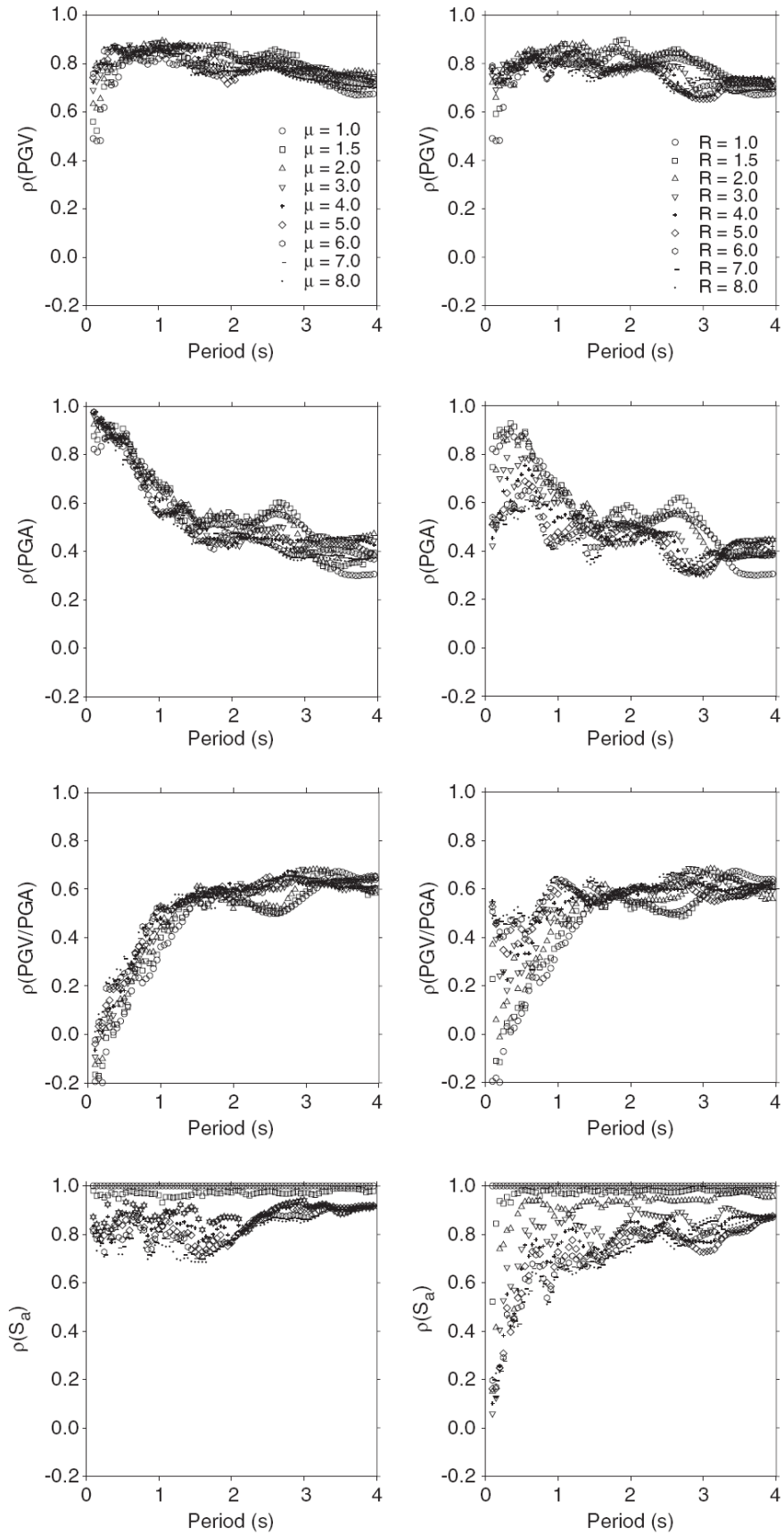


FIGURE 4 CORRELATION OF PGV, PGA, PGV/PGA AND SA WITH SDOF DISPLACEMENT DEMANDS (AKKAR AND ÖZEN, 2005)

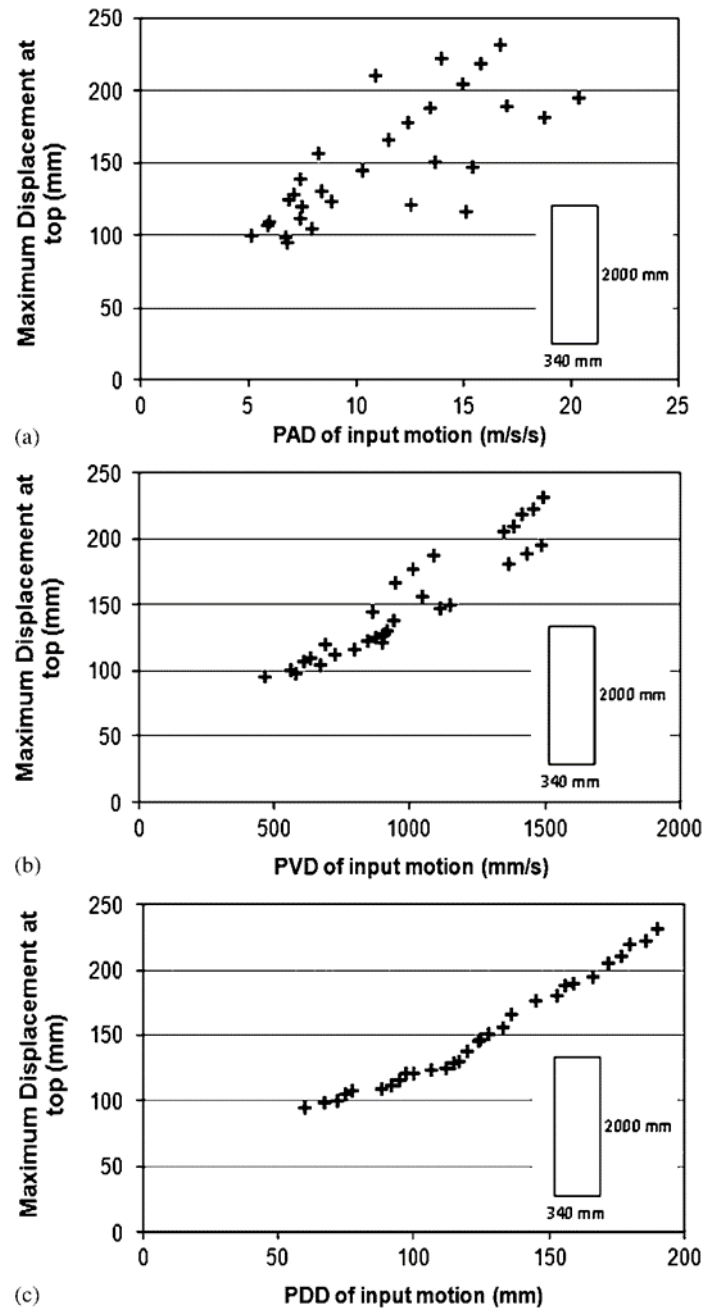


FIGURE 5 CORRELATION OF THE MAXIMUM SPECTRAL ACCELERATION (PAD), MAXIMUM SPECTRAL VELOCITY (PVD) AND MAXIMUM SPECTRAL DISPLACEMENT (PDD) WITH THE MAXIMUM DISPLACEMENT AT THE TOP OF RIGID OBJECTS (KAFLE ET AL., 2011)

Vulnerability functions have also been developed based on the spectral acceleration and spectral displacement. The development was motivated by the fact that PGA cannot represent the frequency content of the ground motions. It has also been facilitated by the emergence of ground-motion prediction equations in terms of spectral ordinates (e.g., Next Generation Attenuation Models developed in Western U.S. (Power et al. (2008)). Singhal and Kiremidjian (1996) used the average acceleration spectral values over various period ranges as intensity measures. Rosetto and Elnashai (2003; 2005) adopted the 5% damped spectral displacement value at the elastic fundamental period as intensity measures and demonstrate that the parameter better correlate with damage than PGA (Figure 3). Wu et al. (2004) investigated the correlations between the observed losses and various intensity measures and concluded that the peak ground velocity (PGV) and spectral acceleration at 1 sec are the most



stable intensity measures. Akkar and Özen (2005) also found that PGV correlates better with deformation demands than other intensity measures (Figure 4).

Kafle et al. (2011) found the maximum spectral displacement correlates best with the top displacement of rigid objects and hence their probability to overturn (Figure 5). The maximum spectral displacement has been adopted as measures of intensity in the study. Colombi et al. (2008) used the inelastic displacement value based on the Substitute Structure approach (Shibata and Sozen, 1976) and the predicted elastic displacement value which was estimated by ground motion prediction equations developed by Facioli et al. (2007).

Earthquake loss modelling packages can be divided into two main categories in relation to the types of parameters chosen to represent ground motion intensity:

1. Intensity based models (e.g., SES 2002 (SES, 2002)) or intensity models which are converted from peak ground acceleration PGA (e.g., EPEDAT (Eguchi et al., 1997))
2. Spectrum based models, which use response spectral ordinates to represent the level of intensity (e.g., HAZUS-MH (FEMA, 2012), LNECLoss (Campos Costa et al., 2010), SELINA (Molina et al., 2010); DBELA (Crowley et al., 2004); EQRM (Robinson et al., 2006)). A simplified spectral shape based on PGA, a short period ordinate (SA at 0.2 sec or 0.3 sec) and long period ordinate (SA at 1.0 sec) is generally adopted.



3. CLASSIFICATION OF BUILDINGS

Classification of buildings is important in earthquake damage loss modelling to ensure a uniform interpretation of results. The classification of buildings has traditionally been done based on the expected earthquake performance of the structures.

The form of construction used for the primary load-bearing structure is generally viewed to be the most important factor affecting the structural performance and is normally used as definition of the buildings classification. As common existing construction types that have often been identified to be seismically vulnerable, masonry and reinforced concrete structures are commonly included in most building classifications in the earthquake damage loss modelling methodologies. For example, Braga et al. (1982) classified buildings into three vulnerability classes (A, B and C): buildings made of fieldstone (type A), or bricks (type B) and of reinforced concrete structures (type C). Masonry and reinforced concrete structures have also been used in earthquake loss estimation methods LESSLoss (Spence, 2007) as shown in Table 1.

The period of constructions has also been identified as a factor influencing the seismic performance of buildings. For more modern buildings, types of load bearing elements are likely to affect the seismic performance of the buildings and hence, they have been included in most building classifications. For example, Spence et al. (1992) have expanded the buildings classification by Braga et al. (1982) to include more information construction materials and building type (Table 2). Similar classification of buildings according to construction types has also been proposed by more recent studies (e.g., Gülkan et al., 1992; Sabetta et al., 1998; Di Pasquale et al., 2005). Meanwhile, Yang et al. (1989) classified buildings into three categories according to the period at which the buildings are constructed. An additional vulnerability class D has also been included by Dolce et al. (2005) to account for reinforced concrete frames or walls with moderate level of seismic design. Grüntal (1998) classified buildings into six vulnerability classes based on construction materials and types of load bearing elements (Table 3).

The seismic performance of buildings is also influenced by the number of storeys, being directly related to the height and hence the natural period of buildings. The number of storeys has also been included in earthquake loss estimation methods and packages. For example, although the range adopted is limited, the number of storeys has been included in the classification of buildings by Rota et al. (2006) (Table 4). The number of storeys has also been included in the classification of buildings adopted by earthquake damage loss estimation packages such as HAZUS MH (FEMA, 2012) as shown in Table 5 and EQRM (Robinson et al., 2006) as shown in Table 6.

In fact, the seismic performance of structures is influenced by many number of factors, such as material properties, buildings dimensions (e.g., storey height, number of storeys, plan dimensions, spacing between frames), structural detailing (e.g., spacing of ties, reinforcement content in longitudinal and transverse directions), and structural irregularities. These factors have been included in the GEM guidelines (D'Ayala et al., 2014) which adopts the



classification of buildings from GEM Taxonomy first level of attributes (Brzev et al., 2012) (Table 7).

TABLE 1 CLASSIFICATION OF BUILDINGS ADOPTED IN LESSLOSS (SPENCE, 2007)

Typologies	Designation	Types
Unreinforced masonry	M1	Rubble stone
	M2	Adobe (earth bricks)
	M3	Simple stone
	M4	Massive stone
	M5	Unreinforced masonry (old bricks)
	M6	Unreinforced masonry – RC floors
Reinforced/confined masonry	M7	Reinforced/confined masonry
Reinforced concrete	RC1	Concrete moment frame
	RC2	Concrete shear walls
	RC3	Dual system

TABLE 2 VULNERABILITY CLASSIFICATION OF BUILDINGS (SPENCE ET AL., 1992)

	MSK Intensity Scale Definition	Main Structural Classification	Building Type	
Non Engineered Buildings	Masonry Type A Weak Masonry	AR Rubble Stone	AR1 Rubble Stone masonry in mud or lime mortar	
		AE Earthen	AE1 Rammed earth constr., earth cob, or solid soil AE2 Composite earth with timber or fibre, wattle and daub, earth and bamboo	
		AA Adobe (Earth brick)	AA1 Adobe sun-dried earth brick in mud mortar	
	Masonry Type B	BB Unreinforced Brick	BB1 Unreinf. Fired Brick Masonry in cement mortar BB2 Brick masonry with horizontal reinforcement	
		Loadbearing unit block masonry	BC Concrete Block	BC1 Concrete Block
	BD Dressed Stone Masonry		BD1 Stone masonry, squared and cut, dimensioned stone, monumental	
	Building Type C Frame Structures	CC RC Frame cast in-situ	CC1 Reinforced Concrete Frame, in-situ	
		CT Timber Frame	CT1 Timber Frame with heavy infill masonry CT2 Timber Frame with timber cladding, Lightweight structure	
	Engineered Buildings	Building Type D Engineered Struct.	DB Reinforced Masonry	DB1 Reinforced Brick Masonry
			DC In-Situ RC Frame	DC1 In-situ RC Frame with non-structural cladding
DC2 In-situ RC Frame with infill masonry				
DC3 In-situ RC Frame with shear wall				
DP Precast RC Structure			DP1 Precast RC Frame with infill masonry	
			DP2 Precast RC Frame with concrete shear walls	
			DP3 Precast Large Panel Structure	
DH Compos. Steel/RC			DH1 Composite steel frame with in-situ RC casing	
DS Steel Frame structures			DS1 Light steel frame	
			DS2 Steel Frame, moment-resistant	
	DS3 Steel frame with infill masonry			
	DS4 Steel frame, braced			
	DS5 Steel frame with RC shear wall or core			



TABLE 3 VULNERABILITY CLASSIFICATION OF BUILDINGS ACCORDING (GRÜNTAL, 1998)

Type of Structure	Vulnerability Class					
	A	B	C	D	E	F
MASONRY	<div style="display: flex; align-items: center;"> <div style="border: 1px solid black; padding: 2px; margin-right: 5px;"> rubble stone, fieldstone adobe (earth brick) </div> <div style="margin-left: 20px;"> </div> <div style="margin-left: 20px; border: 1px solid black; padding: 2px;">Type 1</div> </div>					
	<div style="display: flex; align-items: center;"> <div style="border: 1px solid black; padding: 2px; margin-right: 5px;"> simple stone massive stone </div> <div style="margin-left: 20px;"> </div> <div style="margin-left: 20px; border: 1px solid black; padding: 2px;">Type 2</div> </div>					
	<div style="display: flex; align-items: center;"> <div style="border: 1px solid black; padding: 2px; margin-right: 5px;"> unreinforced, with manufactured stone units </div> <div style="margin-left: 20px;"> </div> </div>					
	<div style="display: flex; align-items: center;"> <div style="border: 1px solid black; padding: 2px; margin-right: 5px;"> unreinforced, with RC floors reinforced or confined </div> <div style="margin-left: 20px;"> </div> <div style="margin-left: 20px; border: 1px solid black; padding: 2px;">Type 3</div> </div>					
	<div style="display: flex; align-items: center;"> <div style="border: 1px solid black; padding: 2px; margin-right: 5px;"> frame without earthquake-resistant design (ERD) </div> <div style="margin-left: 20px;"> </div> <div style="margin-left: 20px; border: 1px solid black; padding: 2px;">RC</div> </div>					
REINFORCED CONCRETE (RC)	<div style="display: flex; align-items: center;"> <div style="border: 1px solid black; padding: 2px; margin-right: 5px;"> frame with moderate level of ERD </div> <div style="margin-left: 20px;"> </div> </div>					
	<div style="display: flex; align-items: center;"> <div style="border: 1px solid black; padding: 2px; margin-right: 5px;"> frame with high level of ERD </div> <div style="margin-left: 20px;"> </div> </div>					
	<div style="display: flex; align-items: center;"> <div style="border: 1px solid black; padding: 2px; margin-right: 5px;"> walls without ERD </div> <div style="margin-left: 20px;"> </div> </div>					
WOOD STEEL	<div style="display: flex; align-items: center;"> <div style="border: 1px solid black; padding: 2px; margin-right: 5px;"> walls with moderate level of ERD </div> <div style="margin-left: 20px;"> </div> </div>					
	<div style="display: flex; align-items: center;"> <div style="border: 1px solid black; padding: 2px; margin-right: 5px;"> walls with high level of ERD </div> <div style="margin-left: 20px;"> </div> </div>					
	<div style="display: flex; align-items: center;"> <div style="border: 1px solid black; padding: 2px; margin-right: 5px;"> steel structures </div> <div style="margin-left: 20px;"> </div> </div>					
WOOD	<div style="display: flex; align-items: center;"> <div style="border: 1px solid black; padding: 2px; margin-right: 5px;"> timber structures </div> <div style="margin-left: 20px;"> </div> </div>					

TABLE 4 CLASSIFICATION OF BUILDINGS (ROTA ET AL., 2006)

Label	Description	No. of storeys
MX1	Mixed	1-2
MX2	Mixed	≥ 3
RC1	Reinforced concrete – seismic design	1-3
RC2	Reinforced concrete – no seismic design	1-3
RC3	Reinforced concrete – seismic design	≥ 4
RC4	Reinforced concrete – no seismic design	≥ 4
IMA1	Masonry – irregular layout – flexible floors – with tie rods	1-2
IMA2	Masonry – irregular layout – flexible floors – w/o tie rods	1-2
IMA3	Masonry – irregular layout – rigid floors – with tie rods	1-2
IMA4	Masonry – irregular layout – rigid floors – w/o tie rods	1-2
IMA5	Masonry – irregular layout – flexible floors – with tie rods	≥ 3
IMA6	Masonry – irregular layout – flexible floors – w/o tie rods	≥ 3

Label	Description	No. of storeys
IMA7	Masonry – irregular layout – rigid floors – with tie rods or tie beams	≥ 3
IMA8	Masonry – irregular layout – rigid floors – w/o tie rods or tie beams	≥ 3
RMA1	Masonry – regular layout – flexible floors – tie rods or tie beams	1-2
RMA2	Masonry – regular layout – flexible floors – w/o tie rods	1-2
RMA3	Masonry – regular layout – rigid floors – with tie rods	1-2
RMA4	Masonry – regular layout – rigid floors – w/o tie rods	1-2
RMA5	Masonry – regular layout – flexible floors – with tie rods	≥ 3
RMA6	Masonry – regular layout – flexible floors – w/o tie rods	≥ 3
RMA7	Masonry – regular layout – rigid floors – with tie rods	≥ 3
RMA8	Masonry – regular layout – rigid floors – w/o tie rods	≥ 3
ST	Steel	all

TABLE 5 CLASSIFICATION OF BUILDINGS ADOPTED IN HAZUS-MH (2012)

No.	Label	Description	Height			
			Range		Typical	
			Name	Stories	Stories	Feet
1	W1	Wood, Light Frame ($\leq 5,000$ sq. ft.)		1 - 2	1	14
2	W2			All	2	24
		Wood, Commercial and Industrial ($> 5,000$ sq. ft.)				
3	S1L	Steel Moment Frame	Low-Rise	1 - 3	2	24
4	S1M		Mid-Rise	4 - 7	5	60
5	S1H		High-Rise	8+	13	156
6	S2L	Steel Braced Frame	Low-Rise	1 - 3	2	24
7	S2M		Mid-Rise	4 - 7	5	60
8	S2H		High-Rise	8+	13	156
9	S3	Steel Light Frame		All	1	15
10	S4L	Steel Frame with Cast-in-Place Concrete Shear Walls	Low-Rise	1 - 3	2	24
11	S4M		Mid-Rise	4 - 7	5	60
12	S4H		High-Rise	8+	13	156
13	S5L	Steel Frame with Unreinforced Masonry Infill Walls	Low-Rise	1 - 3	2	24
14	S5M		Mid-Rise	4 - 7	5	60
15	S5H		High-Rise	8+	13	156
16	C1L	Concrete Moment Frame	Low-Rise	1 - 3	2	20
17	C1M		Mid-Rise	4 - 7	5	50
18	C1H		High-Rise	8+	12	120
19	C2L	Concrete Shear Walls	Low-Rise	1 - 3	2	20
20	C2M		Mid-Rise	4 - 7	5	50
21	C2H		High-Rise	8+	12	120
22	C3L	Concrete Frame with Unreinforced Masonry Infill Walls	Low-Rise	1 - 3	2	20
23	C3M		Mid-Rise	4 - 7	5	50
24	C3H		High-Rise	8+	12	120
25	PC1	Precast Concrete Tilt-Up Walls		All	1	15
26	PC2L	Precast Concrete Frames with Concrete Shear Walls	Low-Rise	1 - 3	2	20
27	PC2M		Mid-Rise	4 - 7	5	50
28	PC2H		High-Rise	8+	12	120
29	RM1L	Reinforced Masonry Bearing Walls with Wood or Metal Deck Diaphragms	Low-Rise	1-3	2	20
30	RM1M		Mid-Rise	4+	5	50
31	RM2L	Reinforced Masonry Bearing Walls with Precast Concrete Diaphragms	Low-Rise	1 - 3	2	20
32	RM2M		Mid-Rise	4 - 7	5	50
33	RM2H		High-Rise	8+	12	120
34	URML	Unreinforced Masonry Bearing Walls	Low-Rise	1 - 2	1	15
35	URMM		Mid-Rise	3+	3	35
36	MH	Mobile Homes		All	1	10



TABLE 6 CLASSIFICATION OF BUILDINGS ADOPTED IN EQRM (ROBINSON ET AL., 2006)

code	description	Stories
W1	timber frame < 5 000 square feet	(1-2)
W2	timber frame > 5 000 square feet	(All)
S1L	steel moment frame	Low-Rise (1-3)
S1M		Mid-Rise (4-7)
S1H		High-Rise (8+)
S2L	steel light frame	Low-Rise (1-3)
S2M		Mid-Rise (4-7)
S2H		High-Rise (8+)
S3	steel frame + cast concrete shear walls	(All)
S4L	steel frame + unreinforced masonry in-fill walls	Low-Rise (1-3)
S4M		Mid-Rise (4-7)
S4H		High-Rise (8+)
S5L	steel frame + concrete shear walls	Low-Rise (1-3)
S5M		Mid-Rise (4-7)
S5H		High-Rise (8+)
C1L	concrete moment frame	Low-Rise (1-3)
C1M		Mid-Rise (4-7)
C1H		High-Rise (8+)
C2L	concrete shear walls	Low-Rise (1-3)
C2M		Mid-Rise (4-7)
C2H		High-Rise (8+)
C3L	concrete frame + unreinforced masonry in-fill walls	Low-Rise (1-3)
C3M		Mid-Rise (4-7)
C3H		High-Rise (8+)
PC1	pre-cast concrete tilt-up walls	(All)
PC2L	pre-cast concrete frames with concrete shear walls	Low-Rise (1-3)
PC2M		Mid-Rise (4-7)
PC2H		High-Rise (8+)
RM1L	reinforced masonry walls + wood or metal diaphragms	Low-Rise (1-3)
RM1M		Mid-Rise (4+)
RM2L	reinforced masonry walls + pre-cast concrete diaphragms	Low-Rise (1-3)
RM2M		Mid-Rise (4-7)
RM2H		High-Rise (8+)
URML	unreinforced masonry	Low-Rise (1-2)
URMM		Mid-Rise (3+)
MH	Mobile homes	(All)

TABLE 7 CLASSIFICATION OF BUILDINGS IN ACCORDANCE WITH GEM TAXONOMY FIRST LEVEL OF ATTRIBUTES (FROM D'AYALA ET AL., 2014)

#	Attribute	Attribute level	Example of ID*
1	Materials of the Lateral Load Resisting System	Material type	MAT99/CR/S/MR/W/MATO....
2	Lateral Load Resisting System	Type of lateral load resisting system	L99/LN/LFM/LFINF...
3	Roof	Roof material	RM/RE/RC/RWO
4	Floor	Floor material	FM/FE/FC/FW...
5	Height	Number of storeys	H99/H:n - H:a,b/HE
6	Date of Construction	Date of construction	Y99/YN/YA/YP
7	Structural Irregularity	Type of irregularity	IR99/IRN/IRH/IRV
8	Occupancy	Building occupancy class	OC99/RES/COM/GOV.....

*Refer to Brezev et al. (2012) for definition of ID



4. DEFINITION OF DAMAGE LEVELS

Earthquake damage loss modelling can be based on empirical and analytical data. For the modelling based on empirical data, ground motion intensity has normally been directly related to building damage. Damage levels of buildings have often been characterised using descriptive damage states. For example, five levels of damage states have been defined and qualitative descriptions for each level have been provided in EMS-98 (Grüntal, 1998) (Figure 6). The damage levels provided in EMS-98 have been adopted in various empirical vulnerability functions (e.g. Dolce et al., 2003; Decanini et al., 2004).

For the modelling based on analytical data, different levels of damage have been commonly related to drifts that have been calibrated to observations of building damages or experimental results (e.g. Singhal and Kiremidjian, 1996; Rossetto and Elnashai, 2005). The GEM guidelines (D'Ayala et al., 2014) defines four structural damage states (Figure 7): Slight (defined as the limit of elastic behaviour), Moderate (corresponds to the peak lateral load bearing capacity), Near Collapse (corresponds to the maximum controlled deformation) and Collapse defined as follows:

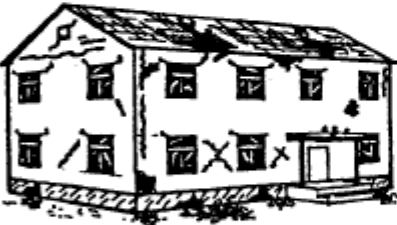
- d_{s1} : represent the attainment of Slight Damage level (SD), it corresponds to the limit of elastic behaviour of the components.
- d_{s2} : represent the attainment of Moderate Damage level (MD), it corresponds to the peak lateral bearing capacity beyond which the structure loses some of its strength or deformation sets in a constant rate of load.
- d_{s3} : represent the attainment of Near Collapse level (NC), it usually correspond to the maximum controlled deformation level for which a determined value of ductility is set.
- d_{s4} : represent the attainment of Collapse level (C).

The different damage states are superimposed on a capacity curve in Figure 8.

The definition of each damage state and inter-storey drifts values associated with each damage state can be obtained from various seismic assessment guidelines such as ATC58-2 (ATC, 2003), Eurocode 8 (CEN, 2004), Vision2000 (SEAOC, 1995) and FEMA-356 (ASCE, 2000). An example of existing definition of limit states is presented in Table 8 and the corresponding inter-storey drift (ID) values is presented in Table 9 for reinforced concrete buildings.

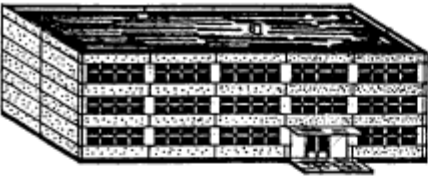
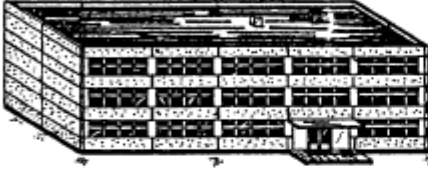
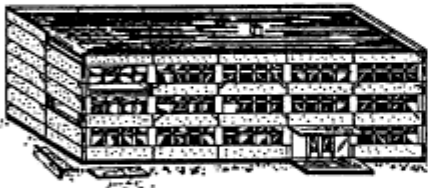
Various definition of damage states have also been proposed in literature. Some of the recommendations for reinforced concrete frames and unreinforced masonry buildings are presented in Tables 10 to 12 showing considerable variations between each recommendation.



Classification of damage to masonry buildings	
	<p>Grade 1: Negligible to slight damage (no structural damage, slight non-structural damage) Hair-line cracks in very few walls. Fall of small pieces of plaster only. Fall of loose stones from upper parts of buildings in very few cases.</p>
	<p>Grade 2: Moderate damage (slight structural damage, moderate non-structural damage) Cracks in many walls. Fall of fairly large pieces of plaster. Partial collapse of chimneys.</p>
	<p>Grade 3: Substantial to heavy damage (moderate structural damage, heavy non-structural damage) Large and extensive cracks in most walls. Roof tiles detach. Chimneys fracture at the roof line; failure of individual non-structural elements (partitions, gable walls).</p>
	<p>Grade 4: Very heavy damage (heavy structural damage, very heavy non-structural damage) Serious failure of walls; partial structural failure of roofs and floors.</p>
	<p>Grade 5: Destruction (very heavy structural damage) Total or near total collapse.</p>

(A) MASONRY BUILDINGS



Classification of damage to buildings of reinforced concrete	
	<p>Grade 1: Negligible to slight damage (no structural damage, slight non-structural damage) Fine cracks in plaster over frame members or in walls at the base. Fine cracks in partitions and infills.</p>
	<p>Grade 2: Moderate damage (slight structural damage, moderate non-structural damage) Cracks in columns and beams of frames and in structural walls. Cracks in partition and infill walls; fall of brittle cladding and plaster. Falling mortar from the joints of wall panels.</p>
	<p>Grade 3: Substantial to heavy damage (moderate structural damage, heavy non-structural damage) Cracks in columns and beam column joints of frames at the base and at joints of coupled walls. Spalling of concrete cover, buckling of reinforced rods. Large cracks in partition and infill walls, failure of individual infill panels.</p>
	<p>Grade 4: Very heavy damage (heavy structural damage, very heavy non-structural damage) Large cracks in structural elements with compression failure of concrete and fracture of rebars; bond failure of beam reinforced bars; tilting of columns. Collapse of a few columns or of a single upper floor.</p>
	<p>Grade 5: Destruction (very heavy structural damage) Collapse of ground floor or parts (e. g. wings) of buildings.</p>

(B) REINFORCED CONCRETE BUILDINGS

FIGURE 6 CLASSIFICATION OF BUILDING DAMAGE ACCORDING TO EMS-98 (GRÜNTAL, 1998)

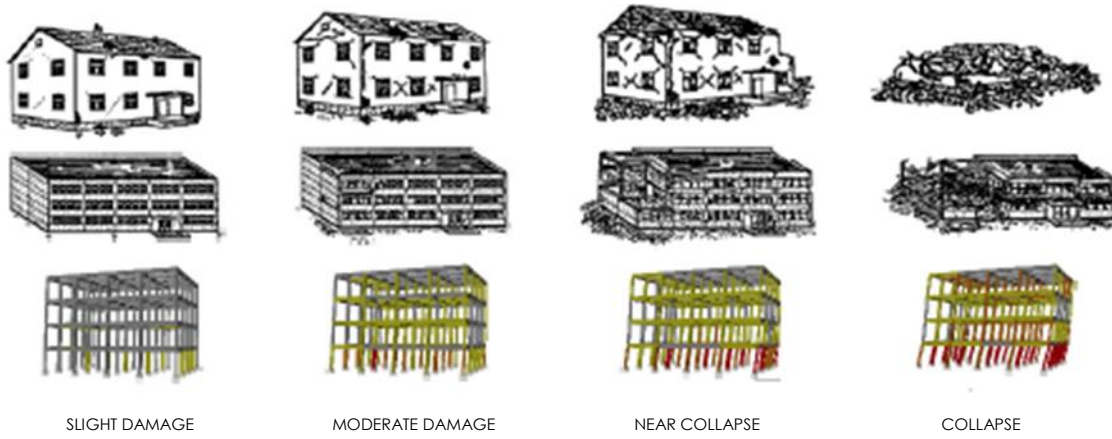


FIGURE 7 DEFINITION OF DIFFERENT DAMAGE STATES (D'AYALA ET AL., 2014)

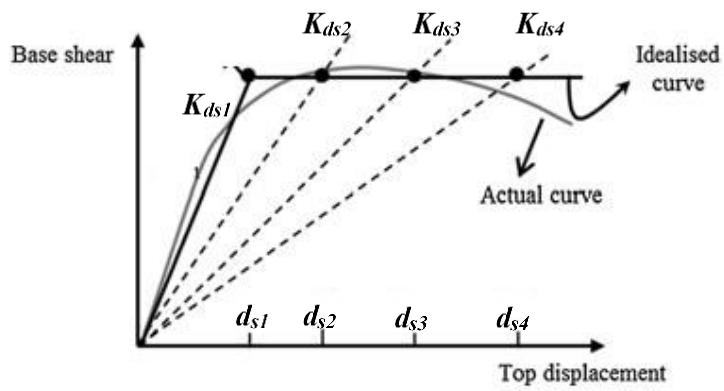


FIGURE 8 CAPACITY CURVE AND DAMAGE LIMIT STATES

TABLE 8 EXAMPLE OF DEFINITION OF DAMAGE STATES ACCORDING TO EXISTING GUIDELINES (D'AYALA ET AL., 2014)

ATC-58 (FEMA P 582012)	Eurocode-8 (CEN 2004)	ATC-58-2 (ATC 2003), Vision 2000 (SEAOC 1995)		ASCE/SEI 41-06 (ASCE 2007); ATC-58-2 (ATC 2003), FEMA-356 (ASCE 2000)		Slight Damage	Moderate Damage	Near Collapse	Collapse	
		Secondary RC Elements	Primary RC Elements	Unreinforced Masonry Infill Walls	Concrete Frames					
Observed damage	Building is considered as slightly damaged. Sustain minimal or no damage to their structural elements and only minor damage to their non-structural components.			Same as primary	Minor hairline cracking (0.02"); limited yielding possible at a few locations; no crushing (strains below 0.003)	Secondary	Primary	Minor (<1/8" width) cracking of masonry infills and veneers; minor spalling in veneers at a few corner openings.	Extensive cracking and hinge formation in ductile elements; limited cracking and/or splice failure in some nonductile columns; joints cracked < 1/8" width	Extensive cracking and crushing; portions of face course shed.
		Secondary	Same as primary.				Extensive cracking and some crushing but wall remains in place; no falling units. Extensive crushing and spalling of veneers at corners of openings.			
	Building is considered as significantly damaged. Extensive damage to structural and non-structural components.	Extensive cracking and hinge formation in ductile elements; limited cracking and/or splice failure in some nonductile columns; severe damage in short columns	Extensive damage to beams: spalling of cover and shear cracking (<1/8") for ductile columns; minor spalling in nonductile columns; joints cracked < 1/8" width	Same as primary.	Secondary	Extensive crushing and shattering; some walls dislodge.	Extensive cracking and hinge formation in ductile elements; limited cracking and/or splice failure in some nonductile columns; severe damage in short columns	Extensive cracking and crushing; portions of face course shed.	Extensive crushing and shattering; some walls dislodge.	Several definition of collapse failure have been proposed
					Primary					



TABLE 9 EXAMPLE OF INTER-STOREY DRIFT VALUES FOR REINFORCED CONCRETE BUILDINGS (ADAPTED FROM D'AYALA ET AL., 2014)

		Slight Damage	Moderate Damage	Near Collapse	Collapse
Vision2000 (SEAOC, 1995); ATC58-2 (ATC, 2003)	Damage State	Light	Moderate	Severe	Complete
	Overall Building Damage	ID	ID < 0.5%	0.5% < ID < 1.5%	1.5% < ID < 2.5%
FEMA-356 (ASCE, 2000); ATC58-2 (ATC, 2003)	Damage State	Light	Moderate	Severe	
	Concrete Frame Elements	ID	1%	2%	4%
	Unreinforced Masonry Infill Wall Elements	ID	0.1%	0.5%	0.6%

TABLE 10 DRIFT RATIOS DEFINING DAMAGE STATES OF LOW-RISE BUILDING TYPES FROM HAZUS-MH (FEMA, 2012)

(A) LOW-RISE

Seismic Design Level	Building Type (Low-Rise)	Drift ratio at the threshold of structural damage			
		Slight	Moderate	Extensive	Complete
High-Code	Concrete moment frame	0.005	0.010	0.030	0.080
Moderate-Code	Concrete moment frame	0.005	0.009	0.023	0.060
Low-Code	Concrete moment frame	0.005	0.008	0.020	0.050
	Unreinforced masonry and concrete moment frame with masonry infill	0.003	0.006	0.015	0.035
Pre-Code	Concrete moment frame	0.004	0.006	0.016	0.040
	Unreinforced masonry and concrete moment frame with masonry infill	0.002	0.005	0.012	0.028

(B) MEDIUM-RISE

Seismic Design Level	Building Type (Low-Rise)	Drift ratio at the threshold of structural damage			
		Slight	Moderate	Extensive	Complete
High-Code	Concrete moment frame	0.0033	0.0067	0.020	0.053
Moderate-Code	Concrete moment frame	0.005	0.0058	0.016	0.040
Low-Code	Concrete moment frame	0.0033	0.0053	0.013	0.033
	Unreinforced masonry and concrete moment frame with masonry infill	0.002	0.004	0.010	0.023
Pre-Code	Concrete moment frame	0.0027	0.0043	0.011	0.027
	Unreinforced masonry and concrete moment frame with masonry infill	0.0016	0.0032	0.008	0.019

(C) HIGH-RISE

Seismic Design Level	Building Type (Low-Rise)	Drift ratio at the threshold of structural damage			
		Slight	Moderate	Extensive	Complete
High-Code	Concrete moment frame	0.0025	0.005	0.015	0.040
Moderate-Code	Concrete moment frame	0.0025	0.0043	0.012	0.030
Low-Code	Concrete moment frame	0.0025	0.004	0.010	0.025
	Unreinforced masonry and concrete moment frame with masonry infill	0.0015	0.003	0.0075	0.0175
Pre-Code	Concrete moment frame	0.002	0.0032	0.008	0.020
	Unreinforced masonry and concrete moment frame with masonry infill	0.0012	0.0024	0.006	0.014



TABLE 11 DEFINING DAMAGE STATES FOR REINFORCED CONCRETE FRAMES

A) ROSETTO AND ELNASHAI (2005)

Damage State	Interstorey Drift (%)
None	0.00
Slight Damage	0.05
Light Damage	0.08
Moderate Damage	0.30
Extensive Damage	1.15
Partial Collapse	2.80
Collapse	>4.36

B) MASI (2004)

Damage State	Definition (EMS-98)	Interstorey Drift (%)
0	Null	<0.1
1	Null	0.1-0.25
2	Slight	0.25-0.5
3	Moderate	0.5-1.0
4	Heavy	1.0-1.5
5	Destruction	>1.5

C) KWON AND ELNASHAI (2006)

Limit States	Interstorey Drift (%)
Serviceability	0.57
Damage Control	1.2
Collapse Prevention	2.3

TABLE 12 DEFINING DAMAGE STATES FOR UNREINFORCED MASONRY BUILDINGS

A) D'AYALA ET AL. (2014)

Limit States	Damage State	Interstorey Drift (%)	
		In-plane failure	Out-of-plane failure
S_{d1}	Slight: cracking limit	0.18-0.23	0.18-0.33
S_{d2}	Structural damage: maximum capacity	0.65-0.90	0.84-0.88
S_{d3}	Near Collapse: loss of equilibrium	1.23-1.92	1.13-2.3
S_{d4}	Collapse	2.0-4.0	2.32-4.0

B) CALVI (1999)

Limit States	Damage State	Interstorey Drift (%)
		In-plane failure
LS1-LS2	No to minor structural damage	0.1
LS3	Significant structural damage	0.3
LS4	Collapse	0.5



5. RELATIONSHIP BETWEEN HAZARD AND THE RESULTING BUILDING DAMAGE

Damage to buildings as a direct result of earthquake induced ground motion has been the focus of studies on earthquake damage loss estimation. Estimates of damage to structures, and consequently loss, are made based on a level of intensity measures (e.g., macroseismic intensity, PGA, spectral parameters). The ground motion intensity is related to damage or losses through fragility and vulnerability functions.

A review of the development of methods for structural vulnerability assessment is provided by Calvi et al. (2006). The assessment techniques can be broadly divided into two categories: empirical methods which are based on observation of damages and analytical methods which rely on assessing structural performance through analytical procedures.

5.1 EMPIRICAL METHODS

The seismic vulnerability assessment of buildings based on empirical methods has been carried out since the early 70's. The probability of damage is presented by: i) damage probability matrices (DPM), which express the probability of damage in a discrete form; ii) continuous vulnerability functions, which express the probability of damage in a continuous function.

5.1.1 Damage Probability Matrices

The use of damage probability matrices for the probabilistic prediction of damage was first proposed by Whittman et al. (1973). The format of DPM is shown in Table 13 where proportion of buildings that are subjected to a certain level of damage was provided for various intensity of earthquake. Eight damage states were proposed based on the extent of damage on structural and non-structural components. The state of damage in DPMs is represented by the damage ratio which is the ratio of cost of repair to cost of replacement, hence DPMs is a form of vulnerability functions. Variations to DPMs have been made based on various macroseismic intensities. For example, Braga et al. (1982) proposed DPM based on the Medvedev–Sponheuer–Karnik (MSK) scale. Di Pasquale et al. (2005) have proposed DPMs based on the MCS (Mercalli Cancani-Sieberg) scale due to the fact that the Italian seismic catalogue is mainly based on the MCS intensity.

Damage probability matrices based on expert judgement and opinion were first introduced in ATC 13 (1985). More than 50 senior earthquake engineering experts were asked to provide low (ML), best (MB) and high (MH) estimates of the damage ratio for Modified Mercalli Intensities (MMI) from VI to XII and 36 building classes. A log normal distribution was assumed for the distribution of the damage ratio with the low and high estimates defining the 5th and 95th percentile, and the best estimates defining the median damage factor (Figure 9). The probability of a central damage factor is determined by calculating the area under the curve of log normal distribution for a certain intensity level and a certain building class.

TABLE 13 EXAMPLE OF DAMAGE PROBABILITY MATRICES PROPOSED BY WHITMAN ET AL. (1973)

Damage State	Structural Damage	Non-structural Damage	Damage Ratio (%)	Intensity of Earthquake				
				V	VI	VII	VIII	IX
0	None	None	0-0.05	10.4	-	-	-	-
1	None	Minor	0.05-0.3	16.4	0.5	-	-	-
2	None	Localised	0.3-1.25	40.0	22.5	-	-	-
3	Not noticeable	Widespread	1.25-3.5	20.0	30.0	2.7	-	-
4	Minor	Substantial	3.5-4.5	13.2	47.1	92.3	58.8	14.7
5	Substantial	Extensive	7.5-20	-	0.2	5.0	41.2	83.0
6	Major	Nearly total	20-65	-	-	-	-	2.3
7	Building condemned		100	-	-	-	-	-
8	Collapse		100	-	-	-	-	-

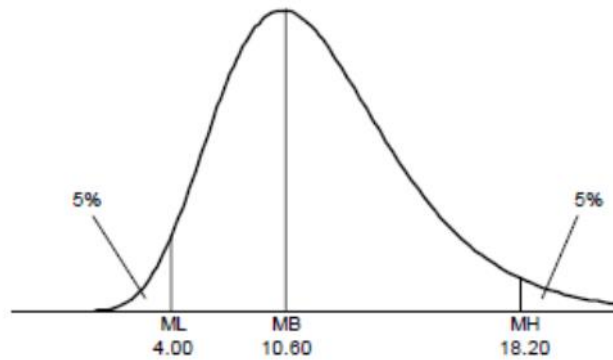


FIGURE 9 EXAMPLE OF A LOGNORMAL DISTRIBUTION OF THE ESTIMATED DAMAGE FACTOR FOR A GIVEN INTENSITY AND CLASS OF BUILDING (MCCORMACK AND RAD, 1997)

Grüntal (1998) proposed damage probability functions based on the EMS-98 macroseismic scale. The building has been classified into four classes (discussed in Section 3). The method uses qualitative description “Few”, “Many” and “Most” and classifies the extent of damage in buildings into five grades. The definition of various damages states have been discussed in Section 4. The intensity was deduced from the qualitative description and the building damage classification as shown in Table 14.

TABLE 14 RELATION BETWEEN THE MSK INTENSITY AND THE NUMBERS OF DAMAGED BUILDINGS FOR VARIOUS VULNERABILITY (GRÜNTAL, 1998)

Intensity	damage	Class A	Class B	Class C	Class D
V	G1	a few	a few		
VI	G1	many	many	a few	
	G2	a few	a few		
VII	G1				a few
	G2		many	a few	
	G3	many	a few		
	G4	a few			
VIII	G2			many	a few
	G3		many	a few	
	G4	many	a few		
	G5	a few			
	G1				
IX	G2				many
	G3			many	a few
	G4		many	a few	
	G5	many	a few		
X	G2				
	G3				many
	G4		most	many	a few
	G5	most	many	a few	
11	G2				
	G3				
	G4			most	many
	G5		most	many	a few
12	G5	All	All	All	most

5.1.2 Vulnerability Index Method

The Vulnerability Index Method (Benedetti and Petrini, 1984; GNDT, 1993) has been used extensively in Italy and is based on a large amount of survey data and observation of past earthquakes. The method uses a field survey form to collect information on important parameters of buildings which could influence their vulnerability. There are 11 parameters including plan and elevation configuration, type of foundation, state of conservation and quality of materials. Each parameter is assigned a scale K_i of 1 to 4 (with 1 being the most optimal to 4 being the most unfavourable) and weighted according to its importance W_i . The vulnerability index (I_v) of each building is evaluated by the following equation (as cited in Calvi et al., 2006):

$$I_v = \sum_{i=1}^{11} K_i W_i \quad (2)$$

The vulnerability index (I_v) ranges from 0 to 382.5, but is generally normalised to 100. 0 represents the least vulnerable buildings and 100 being the most vulnerable. The vulnerability index (I_v) can then be related to a global damage factor (d) of buildings under the same classification, for a given macroseismic intensity or PGA. Global damage factor is defined as the ratio of repair cost to replacement cost. An example of relationship between damage factor, PGA and vulnerability index for a certain typology of building is presented in Figure 10.

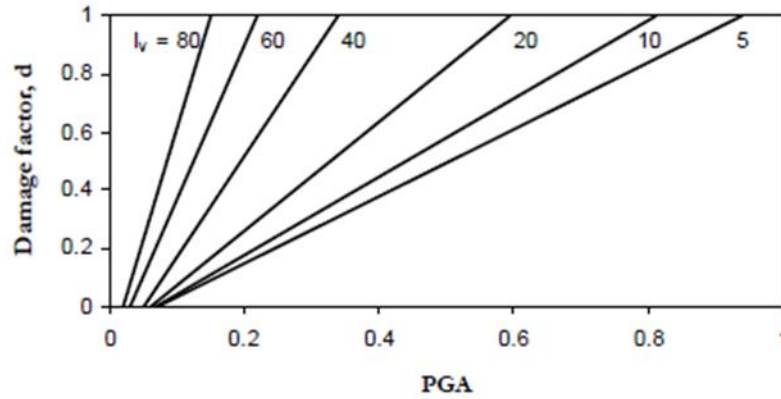


FIGURE 10 VULNERABILITY FUNCTIONS TO RELATE DAMAGE FACTOR (D) AND PEAK GROUND ACCELERATION PGA FOR DIFFERENT VALUES OF VULNERABILITY INDEX (I_v) (GUAGENTI AND PETRINI, 1989)

5.1.3 Continuous vulnerability and fragility functions

Continuous probability functions present the probability of damage of buildings as a continuous function and were introduced later than DPMs. One obstacle of their derivation is due to the fact that macroseismic intensity is not a continuous parameter. Spence et al. (1992) introduced the Parameterless Scale Intensity (PSI), which was used to derive continuous vulnerability functions. The PSI scale has been defined based on the proportion of “brick masonry” buildings experiencing heavy damage (D3) at a particular location. The proportion of the buildings experiencing this state of damage is assumed to follow a Gaussian distribution. The distributions for other states of damage and types of buildings were derived by comparing their performance with the performance of “brick masonry” buildings. The study also attempted to correlate the PSI to ground motion parameters using ground motion acceleration recorded in the vicinity of the damage survey. An example of the vulnerability function based on PSI and MRSA is shown in Figure 11. MRSA is the mean 5% damped response spectral acceleration in period range 0.1 to 0.3 sec averaged between the two horizontal components.

Sabetta et al. (1998) used post-earthquake surveys to derive fragility functions based on ground motion parameters PGA, EPA (Effective Peak Acceleration which is defined as the maximum acceleration between natural period of 0.1 to 0.5 s) and AI (Areas Intensity). A mean normalised damage (p) has been defined per each municipality and class of buildings by the following equation:

$$p = \frac{1}{n} \sum_{i=1}^n d_i N_i / N \quad (3)$$

where n is the number of damage levels, N_i is the number of buildings with damage d_i per municipality and vulnerability class, N is the total number of buildings per municipality and vulnerability class.

The mean normalised damage (p) has been used to obtain empirical fragility functions based on the ground motion parameters, assuming a binomial distribution. The probability of having a damage level k , in a scale of $n + 1$ levels including zero, is given by:

$$f(p, k, n) = \binom{n}{k} p^k (1 - p)^{(n-k)} \quad k = 0, \dots, n \quad (4)$$



Fragility curves have also been derived by Rota et al. (2006) using data obtained from post-earthquake damage surveys. Damage probability matrices were first produced and used to derive fragility functions, assuming lognormal distribution equation (5):

$$f(x) = \frac{1}{x\sigma\sqrt{2\pi}} e^{-\frac{(\ln x - \mu)^2}{2\sigma^2}} \tag{5}$$

The two parameters μ and σ of the lognormal distribution are obtained by fitting the curve into the field data for a single classification and a single damage state. PGA based on the ground motion model by Sabetta and Pugliese (1987) has been adopted as the intensity measures of ground motion shaking.

Vulnerability and fragility functions have been used to relate overall building loss measures (e.g., repair costs) to various intensity measures in earthquake damage loss modelling methodologies such as FEMA-351 (SAC Joint Venture, 2000). An example of the vulnerability curves (in term of percentage of the replacement cost) based on three intensity parameters is presented in Figure 12 compared with damage data obtained from the 1994 Northridge earthquake.

In HAZUS-MH, many of the default fragility relationships are based on the observational method, with fragility curves primarily developed based on California earthquakes.

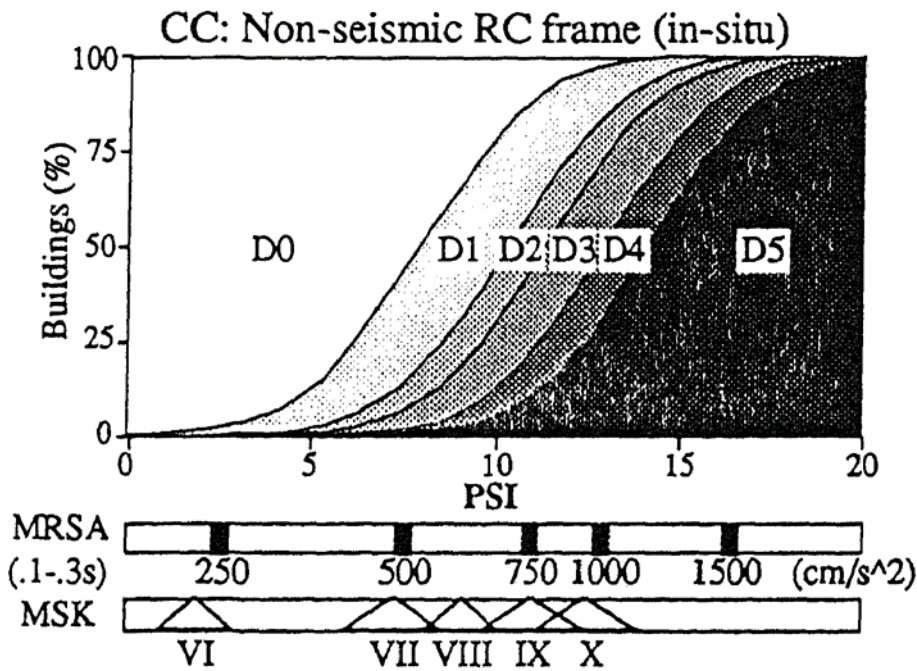


FIGURE 11 VULNERABILITY FUNCTION FOR RC FRAME BASED ON MRSA AND PSI (SPENCE ET AL., 1992)

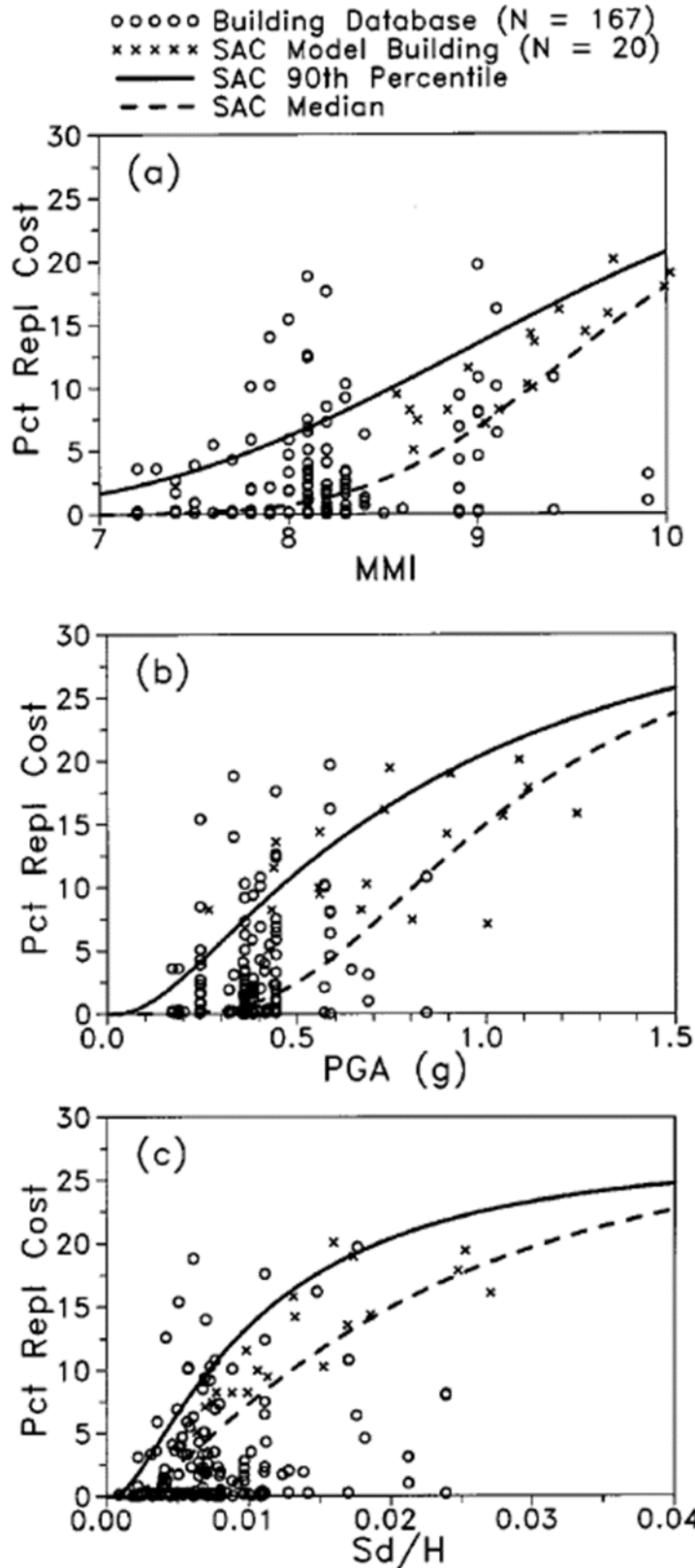


FIGURE 12 EMPIRICAL VULNERABILITY CURVES FROM FEMA-351 (BONOWITZ AND MAISON, 2003)

There are limitations associated with using empirical methods:

- The effects of the ground motion input on the vulnerability are not explicitly modelled in empirical methods.



- It is assumed that the area to be assessed have the same ground conditions of the areas where damages are observed. The derivation of vulnerability functions has normally been done based on a wide range of ground conditions and ground motions which may result in a misrepresentation of damage at a particular site.
- Peak ground acceleration (PGA) may not be a good parameter to represent the earthquake intensity as it does not represent the frequency content of the ground motions. When parameters other than PGA are used (e.g., spectral displacement and spectral acceleration values at the elastic fundamental period of buildings), they are mostly based on ground motion attenuation relationships which also have uncertainties.
- The vulnerability functions are better constrained at moderate damage than high and low damage states due to scarcity of data.
- Vulnerability functions based on empirical methods cannot be used to evaluate retrofit options.

5.2 ANALYTICAL VULNERABILITY FUNCTIONS

The limitations of the empirical methods, the emergence of ground motion prediction equations that provide estimates of spectral values, hazard maps in terms of spectral ordinates as opposed to earthquake intensity and PGA, and the improvement on analytical techniques and computer program capabilities have given rise to analytical methods. Though associated with more uncertainties, empirical methods allow for vulnerability functions to be developed for various types of building stocks and ground motion characteristics. There are four aspects in the construction of vulnerability curves (Figure 13). Some important aspects are described in this section.

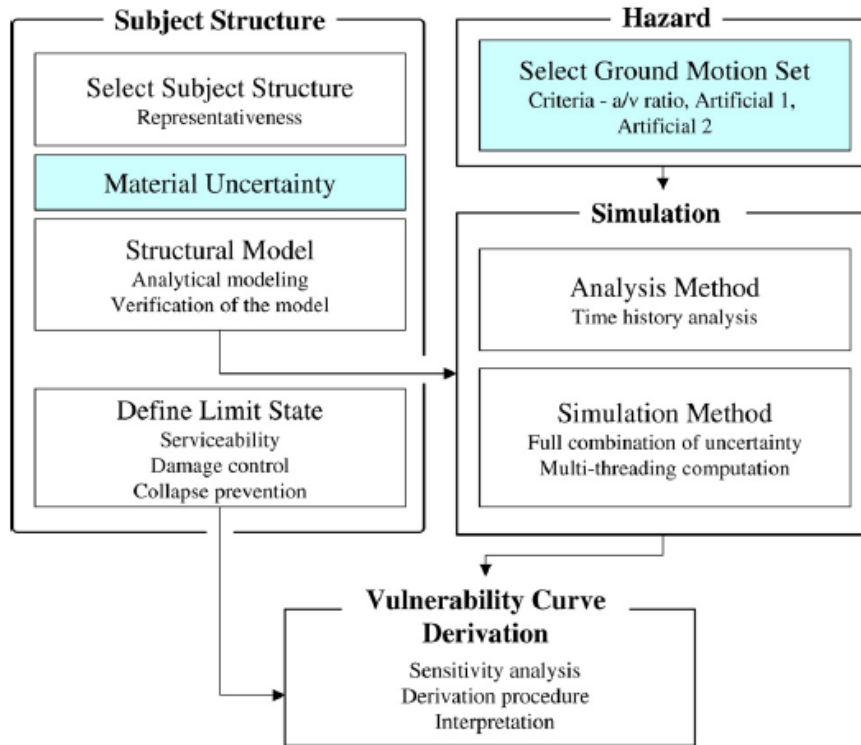


FIGURE 13 TYPICAL FLOW CHART FOR CONSTRUCTION OF ANALYTICAL VULNERABILITY CURVES (KWON AND ELNASHAI, 2006)

5.2.1 Selection of representative building samples

The selection of building samples that will represent a class of buildings is an important step in analytical seismic vulnerability assessment. Most important parameters affecting the selection are the lateral load resisting elements and its material as they highly influence building capacity and seismic response. They are also subjected to considerable scatters due to the quality of workmanships and age of buildings. The GEM guidelines (D'Ayala et al., 2014) recommends three building sampling levels: one index building, three index buildings and multiple index buildings. Each index building, the central, lower and upper bound values (or mean/median and standard deviation values) should be defined to represent the building stock population, which requires some statistical information such as a mean or median value and a standard deviation. Examples of parameters characterising buildings capacity and seismic response (D'Ayala et al., 2014): material properties (strength of material), building dimensions (total height/storey height, number of storeys, plan dimensions), structural detailing and geometric configuration.

In one index building, a median value (or a central value) is set for each parameter affecting the buildings capacity (for example, material properties of lateral load resisting elements) along with the lower and upper bound values. In three index building, each parameter is characterised by three indexes representing typical, poor and good quality with each index further defined by central, lower and upper bound values (Figure 14). In multiple index buildings, the most uncertain characteristics of buildings are sought, such as distribution of building height, the level of base shear used to design the building, the degree of plan irregularities, vertical irregularities, and building height. The shape of the



probabilistic distribution and its statistical information (i.e., mean and standard deviation) are required for each of the building characteristics.

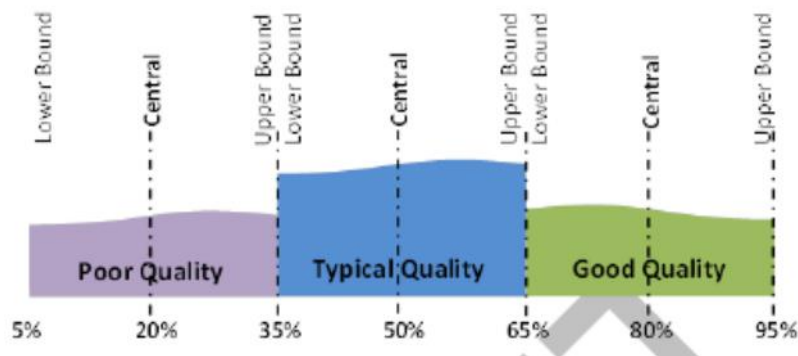


FIGURE 14 DEFINING THREE INDEX BUILDING (D'AYALA ET AL., 2014)

However, due to the computationally intensive nature of analytical seismic vulnerability assessment, existing studies often only consider variation in material properties in their selection of building samples. For example, Singhal and Kiremidjian (1996) derived analytical vulnerability functions for reinforced concrete frames by considering variation in steel yield strength and concrete compressive strength. Similarly, Shinozuka et al. (2000) used variation in compressive strength of concrete and yield strength of steel to construct vulnerability curves for bridges. Masi (2003) derived vulnerability functions for different types of reinforced concrete frames (bare, regularly infilled and pilotis), however considered only variation in reinforcement contents in the structural members.

5.2.2 Choice of analysis methods

Another important step in the derivation of analytical vulnerability functions is the choice of analysis method for evaluating the median and probability distribution of structural responses (i.e. demand) of buildings. Nonlinear dynamic analysis has been adopted by numerous researchers as it is viewed to be able to represent the actual effects of ground motion characteristics (e.g. Singhal and Kiremidjian, 1996; Mosalam et al., 1997; Masi, 2003; Kwon and Elnashai, 2006).

In the GEM guidelines (D'Ayala et al., 2014), analysis options with decreasing order of complexity have been provided: incremental dynamic analysis which is based on nonlinear time history analyses using ground motion inputs that are incremented until either global dynamic or numerical instability occurs and nonlinear static analysis which relies on the capacity curves obtained from pushover analyses. The analysis options are discussed in the next subsections.

5.2.2.1 Incremental Dynamic Analysis

Incremental Dynamic Analysis (IDA) is the dynamic equivalent to a pushover analysis. Non-linear time history analyses were performed using pairs of ground motions that are incremented until either global dynamic or numerical instability occurs in the analysis, indicating that either collapse or large increase in drift associated with small increase in spectral acceleration have occurred. This is illustrated in Figure 13, where the curves in the figure become flat. The median collapse capacity is defined as the value of $S_a(T_1)$ at which 50% of

the ground motion pairs produce numerical instability. The record to record dispersion can be estimated directly from the results of analysis.

The inter-storey drifts at which Slight, Moderate, and Near Collapse damage states occur can be estimated from the progression of local damages in structural elements. The median value of $S_a(T_1)$ for each of the damage state can be inferred directly from the IDA curves (such as that shown in Figure 15).

IDA has been recommended in ATC-63 (FEMA P-695, 2008) and ATC-58 (FEMA P-58, 2012) and has been adopted in various fragility curves produced by various studies (e.g., Kirçil and Polat, 2006; Goulet et al., 2007; Mander et al., 2007; Christovasilis et al., 2009; Rota et al., 2010; Ryu et al., 2011).

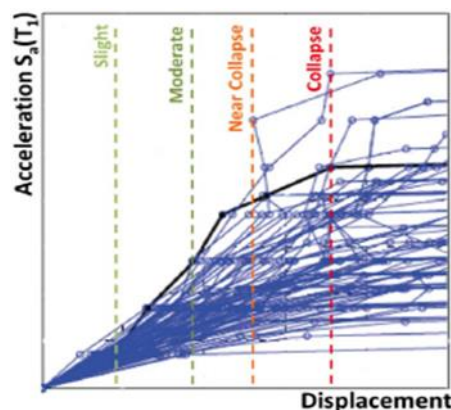


FIGURE 15 EXAMPLE PLOT OF INCREMENTAL DYNAMIC ANALYSIS CURVES (D'AYALA ET AL., 2014)

Nonlinear dynamic analyses are generally computationally intensive especially if numerous analyses are required to represent a building population and ground motion uncertainties. As a result, compromises in regards to the structural modelling were often made. Single-degree of freedom idealisation has often been made (e.g. Ryu et al., 2011; Mander et al., 2007). If a multi-degree of freedom model is adopted, the model normally assumes that buildings are regular in plan and height (e.g., Goulet et al., 2007; Rosetto and Elnashai, 2005).

Three levels of model with decreasing complexity have been recommended in the GEM guidelines (D'Ayala et al., 2014):

1. Multi-degree-of-freedom MDOF model (3D/2D)

The model should include the primary and secondary elements of the building, non-structural components, foundation flexibility, diaphragm action, permanent gravity actions. Various techniques for modelling of frame/shear wall elements, infilled frames and unreinforced masonry walls have been described in the guidelines.

2. Simplified 2D lumped mass MDOF model

Two approaches have been proposed:

- a. Stick models to represent moment resisting frames as shown schematically in Figure 16. When dual systems (systems supported by combination of shear walls and moment resisting frames) are to be modelled, two stick models that are connected by rigid link can be adopted.

b. Single-bay frame

The single-bay frame can be used if there is a need to further distinguish the vertical elements. Each storey is represented by two columns, one connecting beam, and any additional element exists at the storey level (e.g., braces, infills).

3. Single-degree-of-freedom (SDOF) model.

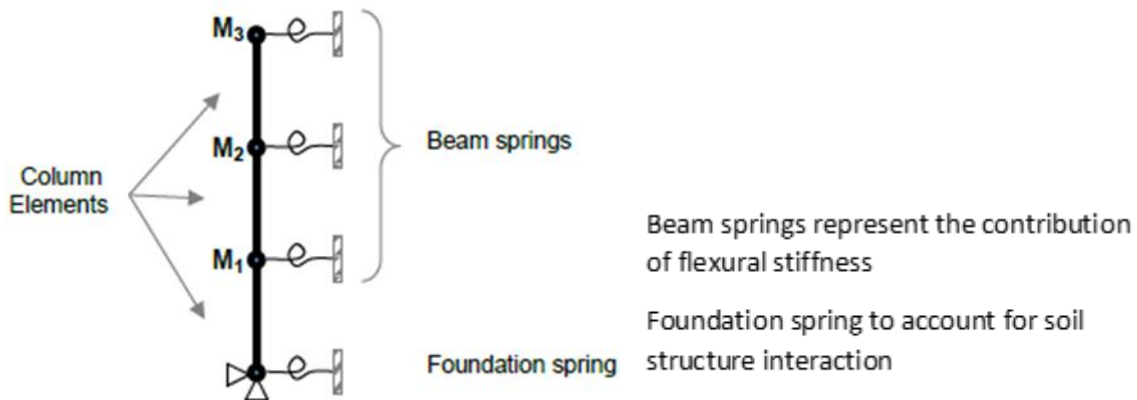


FIGURE 16 2D LUMPED MASS MDOF MODEL (D'AYALA ET AL., 2014)

5.2.2.2 Nonlinear Static Analysis

In an attempt to minimise computational efforts, methods based on nonlinear static procedure have often been adopted. Various approaches have been recommended in the GEM guidelines (D'Ayala et al., 2014) based on the capacity spectrum method and push-over analyses. The capacity spectrum method has been adopted by earthquake loss modelling packages (e.g., HAZUS-MH (FEMA, 2012); LNECLoss (Campos Costa et al., 2010), SELINA (Molina et al., 2010); EQRM (Robinson et al., 2006))

The capacity spectrum method involves comparison between an inelastic response spectrum in acceleration displacement format and a capacity curve of an idealised SDOF system as shown schematically in Figure 17. It consists of the following steps:

1. Perform a push over analysis to develop the relationship between base shear (V_b) and roof displacement (U_N) as shown in Figure 17a.
2. Convert the push over curve to a capacity diagram (Figure 17b), where:

$$\Gamma_1 = \frac{\sum_{j=1}^N m_j \phi_{j1}}{\sum_{j=1}^N m_j \phi_{j1}^2} \quad M_1^* = \frac{(\sum_{j=1}^N m_j \phi_{j1})^2}{\sum_{j=1}^N m_j \phi_{j1}^2} \quad (6)$$

m_j is the lumped mass at the j th floor level, ϕ_{j1} is the value of mode shape at the j th floor for the fundamental mode of vibration, N is the number of floors, and M_1^* is the effective modal mass for the fundamental mode of vibration.

3. Convert the elastic response spectrum with 5% damping from the standard acceleration response format into the acceleration



displacement response format to obtain the demand diagram (Figure 17c) using equation (7):

$$D(T_n) = \frac{T_n^2}{4\pi^2} A(T_n) \quad (7)$$

4. Convert the elastic response spectrum into the inelastic response spectrum. Plot the demand diagram and capacity diagram together to determine the performance point (Figure 17d).

In step 4, the inelastic response spectrum can be determined using a ratio that defines a relationship between the reduction factor (R), the ductility (μ), and the period (T) such as that proposed by Ruiz-Garcia and Miranda (2005) and Dolsek and Fajfar (2004) or using an equivalent linear systems with equivalent natural period (T_{eq}) and equivalent viscous damping (ξ_{eq}) as presented in the ATC-40 (ATC, 1996) and FEMA-274 (ATC, 1997). The performance point is determined using an iteration process whereby the reduction factor R is varied until the intersection point between the inelastic response spectrum and the ductility ratio calculated from the capacity diagram matches with the reduction factor used to derive the intersecting demand curve. In the case when an equivalent linear system is used, an iteration process is carried out by varying the value of ξ_{eq} until the ξ_{eq} of the equivalent linear system matches that used to derive the intersecting the demand curve.

The elastic response spectrum can be derived from ground motion time histories which can match with the target spectrum (as adopted by Rosetto and Elnashai (2005)), ground motion records of an event (as adopted by Uma et al. (2014)), a code spectrum, or ground motion prediction equations (as adopted by earthquake loss models such as HAZUS-MH (FEMA, 2012) and EQRM (Robinson et al., 2006)). The effects of record-to-record dispersion can be incorporated by applying a factor β_D such as that proposed by Ruiz Garcia and Miranda (2007). Some default values of β_D have also been provided in the GEM guidelines (Section 6).

Rosetto and Elnashai (2005) proposed a methodology to produce fragility functions based on the capacity spectrum method. The method allows for the use of suites of ground motion records and hence the method is able to directly evaluate the uncertainties associated with the variability in seismic input. The main difference between the proposed methodology and other capacity spectrum methods is that the demand diagram is not estimated from an iteration process. Instead, the demand diagram is obtained by performing nonlinear dynamic analyses of idealised SDOF models. The methodology is presented schematically in Figure 18. The capacity curve is discretised into a series of points, defined herein as the capacity-demand checking points (CDCP). The capacity curve shape up to each CDCP location defines the elastic period, ductility and nonlinear response curve characteristics of a corresponding SDOF system. The series of SDOF systems associated with each of the CDCPs are subjected to nonlinear dynamic analyses using the ground motion records, to obtain a series of inelastic acceleration and displacement demand values. The demand values correspond to the capacity values of the structure along the radii lines that intersect the capacity curve at the CDCPs. The performance point is the point where the capacity and demand curves intersect. No iteration is required as the inelastic demand and capacity curves have the same ductility.

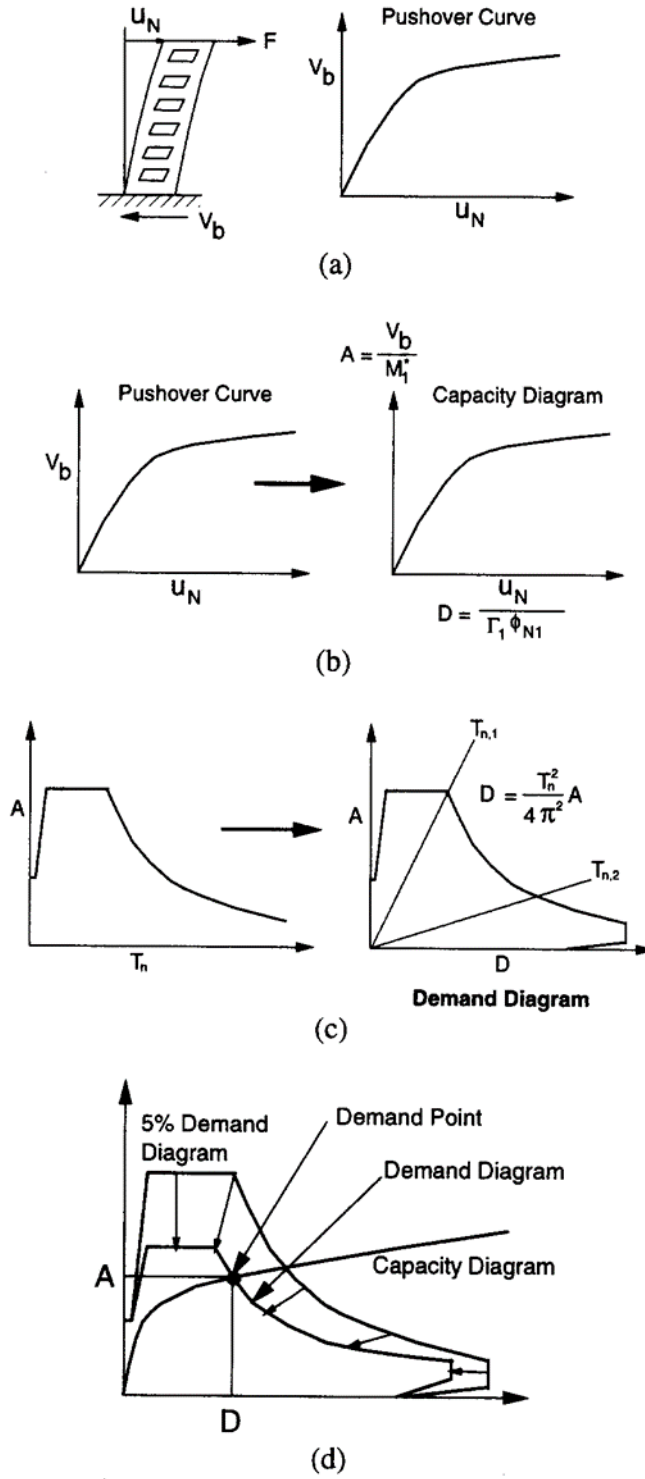


FIGURE 17 CAPACITY SPECTRUM METHOD (CHOPRA AND GOEL, 1999)

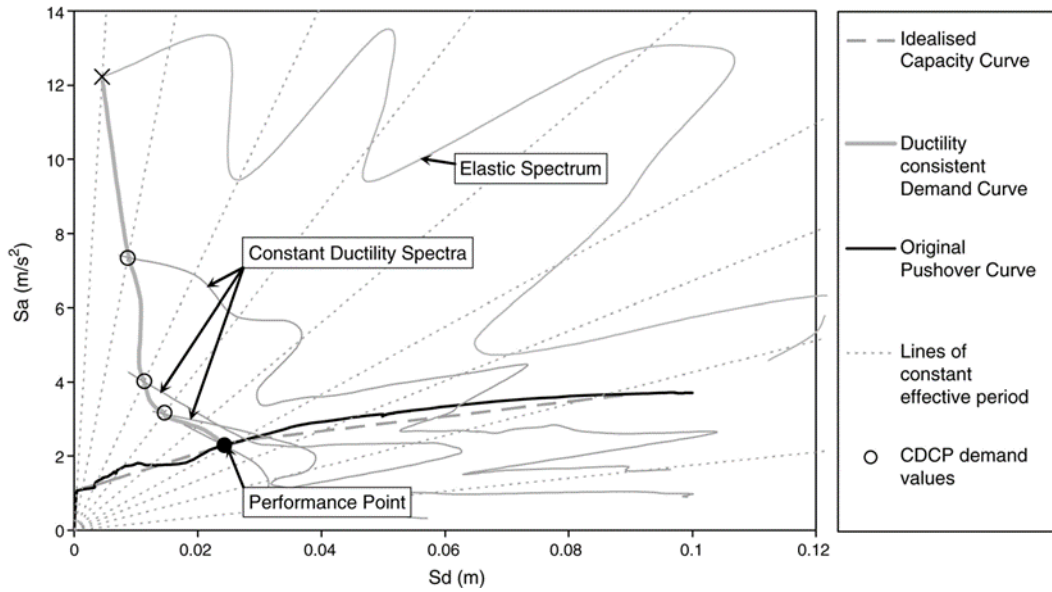


FIGURE 18 ILLUSTRATION OF THE METHOD PROPOSED BY ROSETTO AND ELNASHAI (2005)

Static Push Over to Incremental Dynamic Analysis (SPO2IDA) has been developed by Vamvatsikos and Cornell (2006) to circumvent the computationally intensive nature of Incremental Dynamic Analysis (IDA). SPO2IDA uses empirical relationships from a large database of incremental dynamic analysis results that can be used with static push over analysis curve to obtain estimations for global instability and other damage states. An example of SPO2IDA outputs presented in Figure 19 can be used to obtain the median, 16 and 84 percentile values construct fragility functions for various damage states.

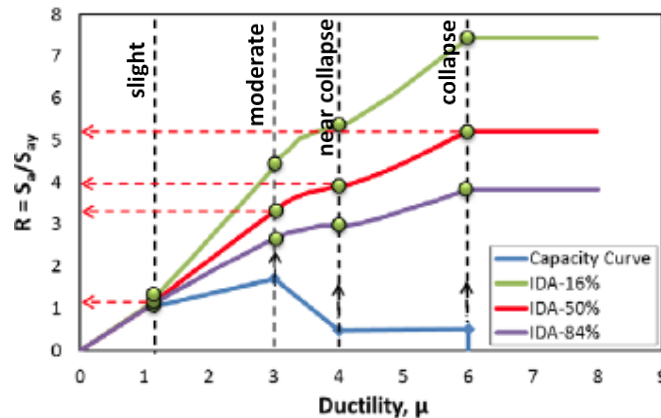


FIGURE 19 EXAMPLE SPO2IDA OUTPUTS FROM VAMVATSIKOS AND CORNELL (2006) AS CITED BY D'AYALA ET AL. (2014)

5.2.3 Selection of Ground Motions

When nonlinear dynamic procedures are adopted, selection of input motions is crucial. The selection of input motions contributes to the uncertainties in vulnerability analyses but there are currently no consistent guidelines on the selection of ground motions for vulnerability assessments. Seismic design guidelines for new buildings such as Eurocode 8 (CEN, 2004) and ASCE/SEI 7-05 (ASCE, 2006) require the use of minimum three sets of ground motions (2 horizontal components or 3 components) for time history analysis. The requirement for three sets of ground motions has also been specified in seismic assessment guidelines for existing buildings such as FEMA-356 (FEMA, 2000) and



ASCE/SEI 41-06 (ASCE, 2007). For calculations of member forces, member inelastic deformations, and storey drifts based on non-linear time history analysis, the seismic design and assessment guidelines recommend seven or more ground motion sets to be used for analysis to obtain the arithmetic mean of the peak response. The maximum value of the peak response should be used fewer than seven ground motions were employed.

The number of ground motion sets required is dependent on factors such as whether mean values or distribution of responses are required, the expected degree of inelastic response and the number of modes contributing significantly to the response quantities. The National Institute of Standards and Technology (NIST) (NEHRP, 2011) recommends taking peak as opposed to mean maximum responses where only three sets of ground motions are used. Seven sets of ground motions are required to obtain the average maximum responses whilst no less than 30 sets of motions are required for construction of fragility curves. 11 sets of ground motions are required to perform incremental dynamic analysis (FEMA P 695, 2008; FEMA P-58, 2012; D' Ayala et al., 2014).

Most guidelines require earthquake ground motion amplitudes to be scaled in order to match a certain target spectrum. Further, the selected records should have magnitudes, fault distances and source mechanisms that are representative of the earthquake scenarios that control the target spectrum (CEN, 2004; ASCE, 2000; FEMA P-58, 2012). There are many ground motion intensity measures which can be used as the basis of selection and scaling of earthquake ground motions. The simplest measures, such as peak ground acceleration, peak ground velocity and peak ground displacement, provide little information on the damage potential of an earthquake ground motion for a specific building. More improved measures are based on elastic response of single-degree-of-freedom (SDOF) system in acceleration, displacement or velocity format. Ground motion intensity measures including inelastic response of SDOF system are able to better characterise the nonlinear response of a building. However, ground motion selection and scaling based on this intensity measures are fairly complex and rarely used in practice.

The most widely used ground motion intensity measures used for selecting and scaling of earthquake ground motions is 5% damped spectral acceleration. Three types of target spectra have been recommended in NIST (NEHRP, 2011):

1. Uniform Hazard Spectrum (UHS)

The UHS is created by probabilistic seismic hazard analysis at many periods in the range of interest without the considerations of hazard at adjacent periods. The UHS is a conservative target spectrum for seismic analysis of buildings as it is highly unlikely that high amplitude spectral values would occur at all periods of a ground motion. An example of UHS is shown in Figure 20 in normal and logarithmic scale.

2. Conditional Mean Spectrum (CMS)

The CMS conditions the entire spectrum on spectral acceleration at a single period specified by users and computes the mean values of spectral acceleration at all other periods. The conditional calculation enables the frequency content of selected ground motions to be



retained. The shape of CMS changes depending on the conditioning period, unlike UHS. The difference between UHS and CMS is shown in Figure 21.

3. Conditional Spectrum

If the CMS select ground motions based on the mean values, the conditional spectrum select ground motions based on both conditional mean and conditional variability.

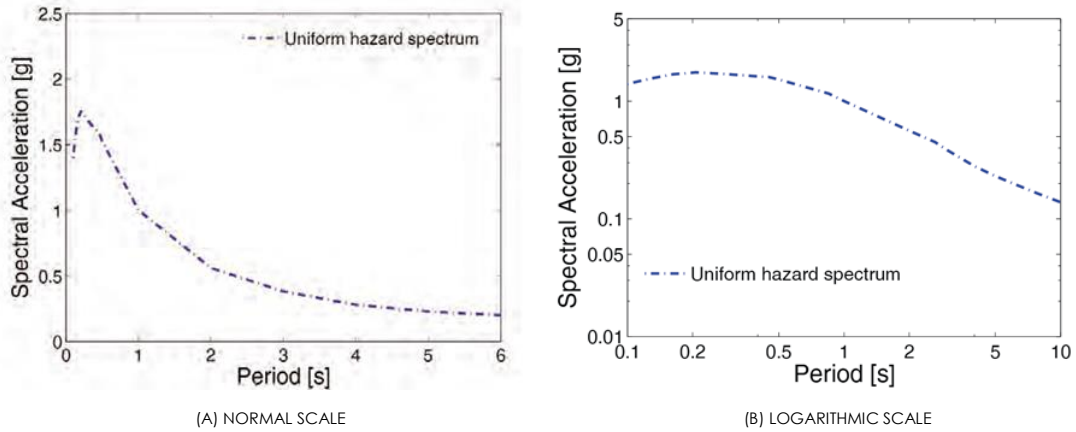


FIGURE 20 UNIFORM HAZARD SPECTRA (NEHRP, 2011)

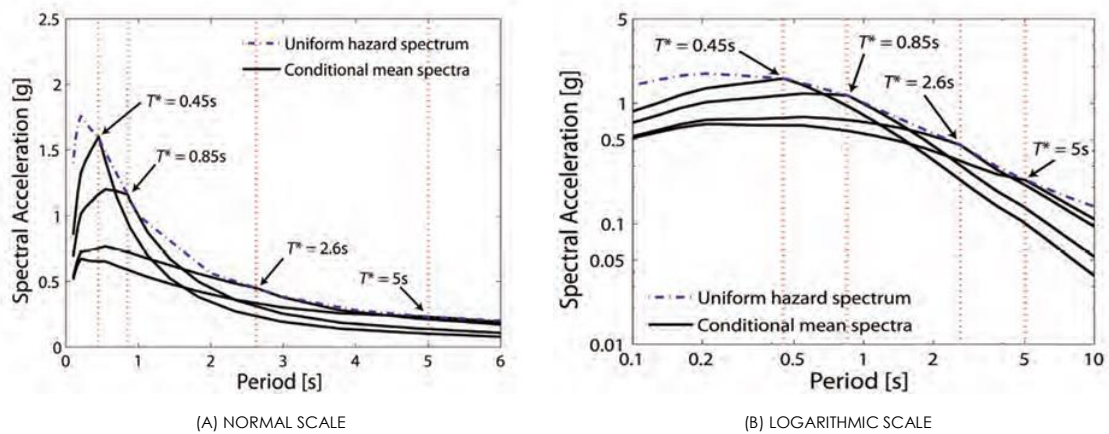


FIGURE 21 CONDITIONAL MEAN SPECTRA ANCHORED AT 0.45 SEC, 0.85 SEC, 2.6 SEC, AND 5 SEC (NEHRP, 2011)

6. CONSTRUCTION OF FRAGILITY CURVES

Fragility curves express the probability of a damage state (ds_i) sustained by an examined building class, being reached or exceeded given a level of ground intensity measures (IM). The curves are commonly assumed to take the form of lognormal cumulative distribution functions having a median value and logarithmic standard deviation:

$$P(DS \geq ds_i | IM) = \Phi \left(\frac{1}{\beta} \ln \left(\frac{IM}{\overline{IM}_{ds_i}} \right) \right) \quad (8)$$

where, $\Phi(\cdot)$ is the cumulative function of the standard normal distribution ($DS | IM$), IM is the median value of demand presented in a form of ground intensity measures, \overline{IM}_{ds_i} is the median capacity corresponding to different damage state, β is the lognormal standard deviation of ($DS | IM$).

The form of lognormal cumulative distribution has been adopted by various seismic vulnerability studies (e.g., Uma et al., 2014; Sokolov and Wenzel, 2011; Kappos et al., 2006; Masi, 2003; Singhal and Kiremidjian, 1996) and earthquake loss modelling packages (e.g., HAZUS-MH (FEMA, 2012); SELINA (Molina et al., 2010); LENECLoss (Campos Costa et al., 2010); EQRM (Robinson et al., 2006)).

The lognormal standard deviation β is the total dispersion parameter and should include: the aleatory uncertainty associated with the randomness in the definition of structural characteristics of structure, uncertainty associated with the mathematical modelling, randomness in earthquake ground motion, and the epistemic uncertainty which arises from building-to-building variability (D'Ayala and Meslem, 2013).

The GEM guidelines (D'Ayala et al. 2014) recommends the lognormal standard deviation for the construction of fragility curves to be taken into account by the following equation:

$$\beta = \sqrt{\beta_D^2 + \beta_M^2} \quad (9)$$

where, β_D is the lognormal standard deviation taking into account uncertainty associated with the demand (record-to-record variability), β_M is the lognormal standard deviation associated with uncertainty in the definition of structural characteristics of buildings, mathematical modelling and building-to-building variability.

The record-to-record variability is estimated directly from the computation when nonlinear dynamic analysis (Section 5.2.2.1) is used to produce the fragility curves. Some default values of β_D provided in the GEM guidelines can be used when nonlinear static procedure (Table 15) is used. The modelling dispersion can be estimated directly from the analysis results if the modelling parameters are defined by lower, central and upper bound values. Some default values of β_M provided in the GEM guidelines can be used if only central value is used to define the modelling parameter. The default values provided in the guidelines have been adopted from ATC-58 (FEMA P-58, 2012) and are presented in Table 15.

HAZUS-MH (FEMA, 2012) defines the lognormal standard deviation for the construction of fragility curves by the following equation:

$$\beta_{Sds} = \sqrt{(\text{CONV}[\beta_C, \beta_D, \bar{S}_{d,Sds}])^2 + (\beta_{M(Sds)})^2} \quad (10)$$

where, β_{Sds} is the lognormal standard deviation that describes the variability for structural damage state (d_s), β_C is the lognormal standard deviation that describes the variability of the capacity curve, β_D is the lognormal standard deviation that describes the variability of the demand spectrum, $\beta_{M(Sds)}$ is the lognormal standard deviation that describes the uncertainty in the estimate of the median value of the threshold of structural damage (d_s). The function "CONV" implies a process of convolving probability distributions of the demand and capacity spectrum. The values of lognormal standard deviation β_{Sds} for reinforced concrete frames and unreinforced masonry buildings recommended in HAZUS-MH (FEMA, 2012) are presented in Table 16.

TABLE 15 THE LOGNORMAL STANDARD DEVIATION VALUES FOR RECORD-TO-RECORD VARIABILITY AND MODELLING UNCERTAINTY (FEMA P-58, 2012)

T_i (sec)	$S = \frac{S_a(T_i)W}{V}$	β_D	β_M
0.2	≤ 1	0.05	0.25
	2	0.35	0.25
	4	0.40	0.35
	6	0.45	0.50
	≥ 8	0.45	0.50
0.35	≤ 1	0.10	0.25
	2	0.35	0.25
	4	0.40	0.35
	6	0.45	0.50
	≥ 8	0.45	0.50
0.5	≤ 1	0.10	0.25
	2	0.35	0.25
	4	0.40	0.35
	6	0.45	0.50
	≥ 8	0.45	0.50
0.75	≤ 1	0.10	0.25
	2	0.35	0.25
	4	0.40	0.35
	6	0.45	0.50
	≥ 8	0.45	0.50
1.0	≤ 1	0.15	0.25
	2	0.35	0.25



	4	0.40	0.35
	6	0.45	0.50
	≥ 8	0.45	0.50
1.5	≤ 1	0.15	0.25
	2	0.35	0.25
	4	0.40	0.35
	6	0.45	0.50
	≥ 8	0.45	0.50
2.0	≤ 1	0.25	0.25
	2	0.35	0.25
	4	0.40	0.35
	6	0.45	0.50
	≥ 8	0.45	0.50

TABLE 16 THE LOGNORMAL STANDARD DEVIATION VALUES σ SDS IN HAZUS-MH (FEMA, 2012)

(A) LOW-RISE

Seismic Design Level	Building Type	Drift ratio at the threshold of structural Damage			
		Slight	Moderate	Extensive	Complete
High-Code	Concrete moment frame	0.81	0.84	0.86	0.81
Moderate-Code	Concrete moment frame	0.89	0.90	0.90	0.89
Low-Code	Concrete moment frame	0.95	0.91	0.85	0.97
	Unreinforced masonry and concrete moment frame with masonry infill	0.99	1.05	1.10	1.08
		1.09	1.07	1.08	0.91
Pre-Code	Concrete moment frame	0.004	0.006	0.016	0.040
	Unreinforced masonry and concrete moment frame with masonry infill	0.002	0.005	0.012	0.028

B) MEDIUM-RISE

Seismic Design Level	Building Type	Drift ratio at the threshold of structural Damage			
		Slight	Moderate	Extensive	Complete
High-Code	Concrete moment frame	0.68	0.67	0.68	0.81
Moderate-Code	Concrete moment frame	0.70	0.70	0.70	0.89
Low-Code	Concrete moment frame	0.70	0.74	0.86	0.98
	Unreinforced masonry and concrete moment frame with masonry infill	0.91	0.92	0.87	0.91
		0.85	0.83	0.79	0.98
Pre-Code	Concrete moment frame	0.0027	0.0043	0.011	0.027
	Unreinforced masonry and concrete moment frame with masonry infill	0.0016	0.0032	0.008	0.019

C) HIGH-RISE

Seismic Design Level	Building Type	Drift ratio at the threshold of structural Damage			
		Slight	Moderate	Extensive	Complete
High-Code	Concrete moment frame	0.66	0.64	0.67	0.78
Moderate-Code	Concrete moment frame	0.66	0.66	0.76	0.91



Low-Code	Concrete moment frame	0.70	0.81	0.89	0.98
	Concrete moment frame with masonry infill	0.71	0.74	0.90	0.97
Pre-Code	Concrete moment frame	0.71	0.80	0.94	1.01
	Concrete moment frame with masonry infill	0.73	0.75	0.91	0.96



7. CONSTRUCTION OF VULNERABILITY CURVES

Vulnerability curves translate the physical damage (depicted by fragility curves) into monetary loss (estimation of repair and reconstruction cost), given a level of ground motion intensity measurement (IM). Two approaches can be used to derive the vulnerability curves: i) Building-based approach.

The vulnerability functions by convolving building level fragility curves with the cumulative cost of a given damage state (d_{si}).

ii) Component-based approach

The vulnerability functions are obtained by correlating the components level-based drifts directly to loss. This approach has been presented in ATC-58 (FEMA P-58, 2012) and is appropriate when vulnerability analysis is performed on a single building

The fragility curves are related to the vulnerability curves by the following relationship (D'Ayala et al., 2014):

$$E(C|IM) = \sum_{i=0}^n E(C|d_{si}) \cdot P(d_{si}|IM) \tag{11}$$

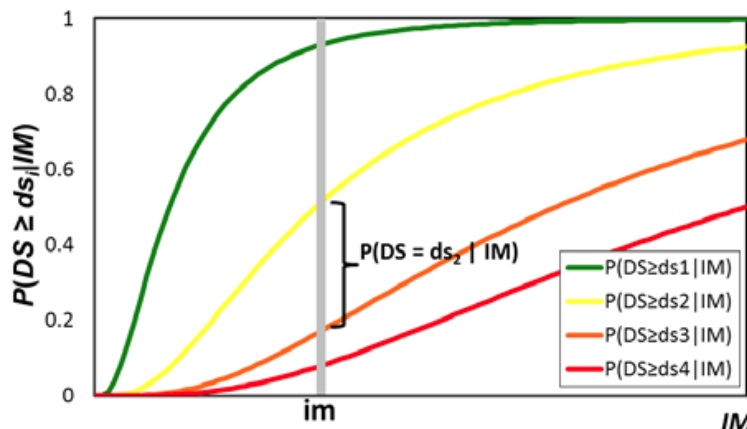
where, n is the number of damage states considered, $P(d_{si}|IM)$ is the probability of a building sustaining damage state d_{si} given ground motion intensity IM , $E(C|d_{si})$ is the complementary cumulative distribution of total repair cost (or loss) given d_{si} , $E(C|IM)$ is the complementary cumulative distribution of total repair cost (or loss) given IM .

The probability of a building sustaining damage state ($P(d_{si}|IM)$) is defined as the distance between two successive fragility curves for a given IM (illustrated in Figure 22).

If local estimates of repair and reconstruction cost are available, the total repair cost, given a damage threshold d_{si} is given by (D'Ayala et al., 2014):

$$E(C|d_{si}) = E(LabCost|Area_{d_{si}}) + E(MatCost|Area_{d_{si}}) \tag{12}$$

where, $E(C|d_{si})$ is the complementary cumulative distribution of total repair cost (or loss) given d_{si} , $E(LabCost|Area_{d_{si}})$ is the local labour cost in the considered region (cost per percentage of damage area), and $E(MatCost|Area_{d_{si}})$ is the local material cost in the considered region (cost per percentage of damage area).



(A) FRAGILITY CURVES CORRESPONDING TO N=4 DAMAGE STATES

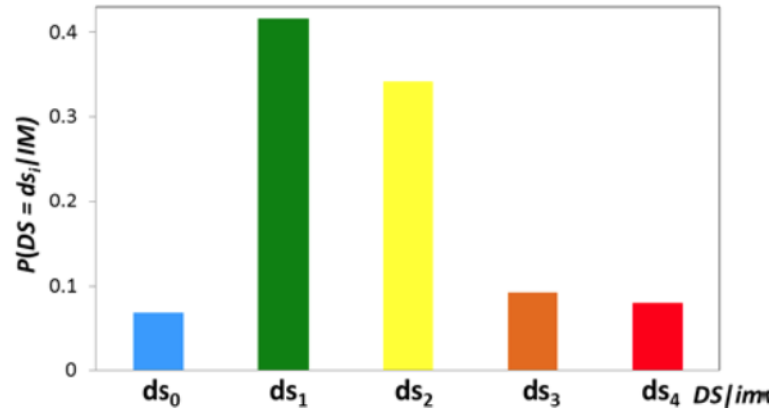
(B) DAMAGE PROBABILITY FOR A GIVEN IM $P(D_{SI} | IM)$

FIGURE 22 CALCULATION OF DAMAGE PROBABILITIES FROM THE FRAGILITY CURVES FOR A SPECIFIC LEVEL OF IM (D'AYALA ET AL., 2014)

Some default values presented in terms of damage factor (DF) have been provided in the GEM guidelines. The recommended DF values have been collated from literature (e.g., FEMA, 2003; Di Pasquale et al., 2005; Dolce et al., 2006) and included the material and labour cost for structural and non-structural components. The DF values are presented as a function of building typology and building occupancy class (in the case of HAZUS (FEMA, 2003)). Given the DF values, the total repair cost can be calculated by:

$$E(C|d_{si}) = DF_{d_{si}} CC \quad (13)$$

where, CC is the Construction Cost in the considered region.

Repeating the process of calculations using equations (11) and (12) or equations (11) and (13) for a range of values of intensity measures results in vulnerability curves.



8. SUMMARY

This report presents a review of existing methodologies on earthquake damage loss modelling. Earthquake damage loss modelling provides estimates of loss due to certain hazard intensity. The estimations are generally presented in terms of fragility functions which translates values of ground motion intensity measures into values of some damage measures (e.g., displacement, acceleration, inter-storey drifts) or vulnerability functions which translate the ground motion intensity measures directly into values of the decision variables (e.g., monetary loss, number of buildings subjected to certain level of damage).

The earthquake loss damage modelling requires: 1. intensity of hazards, 2. classification of building data, 3. damage state, and 4. relationship between hazard and the resulting building damage, to be defined.

Ground motions in the earthquake damage loss modelling are commonly defined using deterministic analysis (based on a single earthquake scenario), or probabilistic analysis (based on aggregation of a number of earthquake scenarios). Site effects are normally incorporated using: calculation of the full transfer function, modification of bedrock ground motion by frequency dependent factors, or modification of bedrock ground motion by frequency independent factors. Uncertainties associated with ground motion modelling, including the modelling of site effects, have significant influence on the loss estimation. Hence their treatment is a major component of the earthquake damage loss modelling.

Macroseismic intensity has traditionally been adopted as a ground motion intensity measure. However, macroseismic intensity scales are derived primarily from observations of damage. Hence, the probability of damage resulting from the earthquake loss modelling is not totally independent of the measure of ground intensity. Other ground motion parameters such as peak ground acceleration and effective peak acceleration have been adopted. Vulnerability functions have also been developed based on spectral values, such as spectral acceleration and spectral displacement as they have often been found to correlate better with damages.

Classification of buildings and definition of damage levels are important aspects in earthquake damage loss modelling. The classification of buildings has traditionally been done based on construction forms, but more recently been extended to include types of load bearing elements and number of storeys. Seismic performance of structures is in fact influenced by number of factors such as material properties, buildings dimensions, structural detailing, and structural irregularities. However, classification of buildings in practice rarely incorporates all of these factors due to the complexity involved in obtaining all the building data. Each classification of buildings is related to damage levels. The classification of damage levels can be related directly to damage states or related to drifts that have been calibrated to building damages.

Hazard is generally related to building damage through fragility functions and vulnerability functions. Selection of representative buildings, choice of analysis methods and selection of ground motions are important aspects in seismic vulnerability assessments to produce fragility and vulnerability functions. There



are few factors which affect the seismic performance of buildings (e.g., material properties, building dimensions, structural detailing, the degree of plan irregularities, vertical irregularities, and building height). However, due to the computationally intensive nature of seismic vulnerability assessments, existing studies often only consider variation in material properties in their selection of building samples. In terms of the choice analysis methods, nonlinear dynamic analysis is generally considered to be able to represent the actual effects of ground motion characteristics and have been adopted in numerous studies. However, nonlinear dynamic analysis is computationally expensive and as a result, compromises in regard to the structural modelling were often made. As a result, SDOF and simplified MDOF models have normally been adopted in seismic vulnerability assessment methodologies. In an attempt to minimise computational efforts, nonlinear static procedures based on the capacity spectrum method have also been adopted. When nonlinear dynamic analysis is used, selection and scaling of input ground motions is crucial. There are no consistent guidelines on the number of ground motions are required and how they should be selected and scaled. However, three sets of ground motions are often recommended when the maximum value of the results is used, whilst seven sets are recommended when the mean value is used. 30 sets of ground motions are recommended for the construction of fragility curves. The selected ground motions are generally scaled based on either uniform hazard or conditional spectrum.

From analyses of building samples in a certain building class under the selected ground motions, fragility curves can be constructed. Fragility curves express the probability of a damage state sustained by an examined building class, being reached or exceeded given a level of ground intensity measures. The curves are commonly assumed to take the form of lognormal cumulative distribution functions having a median value and logarithmic standard deviation. The fragility curves are related to the vulnerability curves through estimates of total repair cost.



REFERENCES

- Abrahamson, N.A. and Bommer, J.J. (2004), "Probability and uncertainty in seismic hazard analysis", *Earthquake Spectra* 21 (2): 603–607.
- Abrahamson, N.A. and Youngs, R.R. (1992), "A stable algorithm for regression analyses using the random effects model", *Bulletin of Seismological Society of America* 82(1): 505–510.
- Akkar, S., Ozen, Ö. (2005), "Effect of peak ground velocity on deformation demands for SDOF systems", *Earthquake Engineering and Structural Dynamics* 34(13): 1551-1571.
- American Society of Civil Engineers (ASCE) (2007), *Seismic Rehabilitation of Existing Buildings*, ASCE/SEI 41-06, American Society of Civil Engineers, Reston, Virginia.
- American Society of Civil Engineers (ASCE) (2006), *Minimum Design Loads for Buildings and Other Structures*, ASCE/SEI7-05, American Society of Civil Engineers, Reston, Virginia.
- American Society of Civil Engineers (2000), *Prestandard and commentary for the seismic rehabilitation of buildings*. FEMA-356, Washington, D.C.
- Applied Technology Council (1985), *Earthquake damage evaluation data for California*, ATC-13.
- Applied Technology Council (1996), *Seismic evaluation and retrofit of concrete buildings*, Vol. 1, ATC-40
- Applied Technology Council (1997), *Earthquake damage and loss estimation methodology and data for Salt Lake County, Utah*, ATC-36.
- Applied Technology Council (ATC) (1997), *NEHRP Commentary on the Guidelines for the Seismic Rehabilitation of Buildings*, prepared for the Building Seismic Safety Council, FEMA-274, Washington, D.C.
- Applied Technology Council (ATC) (2003), *Preliminary Evaluation of Methods for Defining Performance*, ATC-58-2, Redwood City, CA.
- Benedetti, D., Petrini, V. (1984), "Sulla Vulnerabilità Di Edifici in Muratura: Proposta Di Un Metodo Di Valutazione", *L'industria delle Costruzioni* 149(1): 66-74.
- Blume, J.A., Scholl, R.E., Lum, P.K. (1977). *Damage factors for predicting earthquake dollar loss probabilities*, URS/John A. Blume Engineers, for the U.S. Geological Survey.
- Bommer, J.J. and Crowley, H. (2006), "The influence of ground motion variability in earthquake loss modelling", *Bulletin of Earthquake Engineering* 4:231–248.
- Bommer, J.J., Scherbaum, F., Bungum, H., Cotton, F., Sabetta, F. and Abrahamson, N.A. (2005), "On the use of logic trees for ground-motion prediction equations in seismic hazard analysis", *Bulletin of the Seismological Society of America* 95(2), 377–389.
- Bommer, J.J., Spence, R., Erdik, M., Tabuchi, S., Aydinoglu, N., Booth, E., del Re, D. and Peterken, O. (2002), "Development of an earthquake loss model for Turkish catastrophe insurance", *Journal of Seismology* 6(3): 431–446.



- Bonowitz, D., Maison, B.F. (2003), "Northridge welded steel moment-frame damage data and its use for rapid loss estimation", *Earthquake Spectra* 19(2): 335-364.
- Braga, F., Dolce, M. and Liberatore, D. (1982). "A statistical study on damaged buildings and an ensuing review of the MSK-76 scale", Proceedings of the Seventh European Conference on Earthquake Engineering, Athens, Greece, pp. 431–450.
- Brzev, S., Scawthorn, C., Charleson, A.W., Jaiswal, K. (2012), GEM basic building taxonomy, Report produced in the context of the GEM Ontology and Taxonomy Global Component project, 45 pp.
- Campos Costa, A., Sousa, M.L., Carvalho, A., Coehlo, E. (2010), "Evaluation of seismic risk and mitigation strategies for the existing building stock: application of LNECloss to the metropolitan area of Lisbon", *Bulletin of Earthquake Engineering* 8:119–134.
- European Committee for Standardization (CEN) (2004). Design of structures for earthquake resistance, Part 1: General rules, seismic actions and rules for buildings, Eurocode08, ENV 1998-1-1, Brussels, Belgium.
- Calvi, G.M., Pinho, R., Magenes, G., Bommer, J.J., Restrepo-Velez, L.F., Crowley, H. (2006), "Development of seismic vulnerability assessment methodologies over the past 30 years", *SET Journal of Earthquake Technology* 472(3): 75-104.
- Chan, L.S., Chen, Y., Chen, Q., Chen, L, Liu, J., Dong, W., Shah, H. (1998). "Assessment of Global Seismic Loss Based on Macroseismic Indicators", *Natural Hazards* 17: 269–283.
- Chandler, A.M., Lam, N.T.K., Sheikh, M.N. (2002), "Response spectrum predictions for potential near-field earthquakes affecting Hong Kong", *Soil Dynamics and Earthquake Engineering* 22(6): 419–440.
- Chen, Q.F., Mi, H.L., Huang, J. (2005), "A simplified approach to earthquake risk in mainland China", *Pure and Applied Geophysics* 162(6-7): 1255-1269.
- Chopra, A.K., Goel, R.K. (1999), "Capacity-demand-diagram method based on inelastic design spectrum", *Earthquake Spectra* 15(4): 637–656.
- Christovasilis, I.P., Filiatrault, A., Constantiou, M.C., Wanitkorkul, A. (2009), "Incremental dynamic analysis of woodframe buildings", *Earthquake Engineering and Structural Dynamics* 38: 477-496.
- Colombi, M., Borzi, B., Crowley, H., Onida, M., Meroni, F., Pinho, R. (2008). "Deriving vulnerability curves using Italian earthquake damage data", *Bulletin of Earthquake Engineering* 6: 485–504.
- Crowley, H. and Bommer, J.J. (2006), "Modelling seismic hazard in earthquake loss models with spatially distributed exposure", *Bulletin of Earthquake Engineering* 4: 249–273.
- Crowley, H., Pinho, R., Bommer, J.J. (2004), "A probabilistic displacement-based vulnerability assessment procedure for earthquake loss estimation", *Bulletin of Earthquake Engineering* 2(2): 173 – 219.
- Crowley, H., Bommer, J.J., Pinho, R., Bird, J. (2005), "The impact of epistemic uncertainty on an earthquake loss model", *Earthquake Engineering and Structural Dynamics* 34: 1653 – 1685.



- Crowley, H., Monelli, D., Pagani, M., Silva, V., Weatherill, H. (2013), OpenQuake engine user instruction manual, GEM foundation. Available from: http://www.globalquakemodel.org/media/cms_page_media/79/oa-manual-1_0.pdf
- D' Ayala, D., Meslem, A., 2013a. Guide for selection of existing fragility curves and compilation of the database, GEM Technical Report 2013-X, GEM Foundation.
- D' Ayala, D., Meslem, A., Vamvatsikos, D., Porter, K., Rossetto, T., Crowley, H., Silva, V. (2014). Guidelines for analytical vulnerability assessment of low/mid-rise buildings - Methodology, Vulnerability Global Component project. Available from: www.nexus.globalquakemodel.org/gem-vulnerability/posts/
- Decanini, L., De Sortis, A., Goretti, A., Liberatore, L., Mollaioli, F., Bazzurro, P. (2004). "Performance of reinforced concrete buildings during the 2002 Molise, Italy, Earthquake", *Earthquake Spectra* 20(S1): S221–S255.
- Di Pasquale, G., Orsini, G., Romeo, R.W. (2005). "New developments in seismic risk assessment in Italy", *Bulletin of Earthquake Engineering* 3(1): 101–128.
- Dolce, M., Masi, A., Marino, M., Vona, M. (2003). "Earthquake damage scenarios of the building stock of Potenza (Southern Italy) including site effects", *Bulletin of Earthquake Engineering* 1(1): 115–140.
- Dolsek, M., Fajfar, P., (2004), "Inelastic spectra for infilled reinforced concrete frames", *Earthquake Engineering and Structural Dynamics* 33: 1395–1416.
- Eguchi, R.T., Goltz, J.D., Seligson, H.A., Flores, P.J., Blais, N.C., Heaton, T.H., Bortugno, E. (1997), "Real-Time Loss Estimation as an Emergency Response Decision Support System: The Early Post-Earthquake Damage Assessment Tool (EPEDAT)." *Earthquake Spectra* 13(4): 815-832.
- Faccioli, E., Cauzzi, C., Paolucci, R., Vanini, M., Villani, M., Finazzi, D. (2007). "Long period strong motion and its uses input to displacement based design", Proceedings of the 4th international conference on earthquake geotechnical engineering, Thessaloniki, Greece.
- Federal Emergency Management Agency (FEMA) (2012). HAZUS-MH 2.1 Technical Manual. Federal Emergency Management Agency, Washington D.C.
- Federal Emergency Management Agency FEMA P-58 (2012), Seismic Performance Assessment of Buildings, ATC-58, Applied Technology Council, Washington, D.C.
- Federal Emergency Management Agency (FEMA) (2009), Quantification of Building Seismic Performance Factors, FEMA P-695 Report, prepared by Applied Technology Council for Federal Emergency Management Agency, Washington, D.C.
- Federal Emergency Management Agency (FEMA) (2003), HAZUS-MH - Multi-hazard loss estimation methodology, Technical and user's manual, Washington DC.
- Federal Emergency Management Agency (FEMA) (2000), Prestandard and commentary for the seismic rehabilitation of buildings, FEMA-356, prepared by the American Society of Civil Engineers for the Federal Emergency Management Agency, Washington, D.C.



- Goulet, C.A., Haselton, C.B., Mitrani-Reiser, J., Beck, J.L., Deierlein, G.G., Porter, K.A., Stewart, J.P. (2007), "Evaluation of the seismic performance of a code-conforming reinforced-concrete frame building—from seismic hazard to collapse safety and economic losses", *Earthquake Engineering and Structural Dynamics* 2007: 1973-1997.
- GNDT (1993), "Rischio Sismico Di Edifici Pubblici, Parte I: Aspetti Metodologici", Proceedings of CNR-Gruppo Nazionale per la Difesa dai Terremoti, Roma, Italy.
- Guagenti, E., Petrini, V. (1989), "The case of old buildings: towards a damage-intensity relationship", Proceedings of the Fourth Italian National Conference on Earthquake Engineering, Milan, Italy (in Italian).
- Gülkan, P., Sucuoğlu, H., Ergünay, O. (1992), "Earthquake vulnerability, loss and risk assessment in Turkey", Earthquake Engineering, Tenth World Conference, Balkema, Rotterdam.
- Insurance Services Office (1983). Guide for determination of earthquake classifications. New York, NY: ISO.
- Kafle, B., Lam, N.T.K., Gad, E.F., Wilson, J.L. (2011), "Displacement controlled rocking behaviour of rigid objects", *Earthquake Engineering and Structural Dynamics* 40: 1653–1669.
- Kalkan, E., Wills, C.J., Branum, D.M. (2010), "Seismic hazard mapping of California considering site effects", *Earthquake Spectra* 26(4): 1039–1055.
- Kappos, A.J., Panagopoulos, G., Panagiotopoulos, C., Penelis, G. (2006), "A hybrid method for the vulnerability assessment of R/C and URM buildings", *Bulletin of Earthquake Engineering* 4: 391–413.
- Kirçil, M.S., Polat, Z (2006), "Fragility analysis of mid-rise R/C frame buildings", *Engineering Structures* 28:1335-1345.
- KOERI2002 (2002), Earthquake risk assessment for Istanbul Metropolitan Area, Bogazici University, Kandilli Observatory and Earthquake Research Institute, Istanbul, Rep. no. 16, <http://www.koeri.boun.edu.tr/depremmuh/EXECENG.pdf>, 2002.
- Kwon, O. and Elnashai, A. (2006). "The effect of material and ground motion uncertainty on the seismic vulnerability curves of RC structure", *Engineering Structures* 28: 289–303.
- Masi, A. (2003). "Seismic vulnerability assessment of gravity load design R/C frames", *Bulletin of Earthquake Engineering* 1: 371–395.
- Mander, J.B., Dhakal, R.P., Mashiko, N., Solberg, K.M. (2007), "Incremental dynamic analysis applied to seismic financial risk assessment of bridges", *Engineering Structures* 29: 2662-2672.
- McCormack, T.C., Rad, F.N. (1997), "An earthquake loss estimation methodology for buildings based on ATC-13 and ATC-21", *Earthquake Spectra* 13(4): 605-621.
- McGuire, R.K., Cornell, C.A. and Toro, G.R. (2005), "The case for using mean seismic hazard", *Earthquake Spectra* 21(3): 879–886.



- Molina, S. and Lindholm, C. (2005). "A logic tree extension of the capacity spectrum method developed to estimate seismic risk in Oslo, Norway", *Journal of Earthquake Engineering* 9(6): 877–897.
- Molina, S., Lang, D.H., Lindholm, C.D. (2010), "SELENA - An open-source tool for seismic risk and loss assessment using a logic tree computation procedure", *Computers & Geosciences* 36: 257–269.
- Mosalam, K.M., Ayala, G., White, R.N., Roth C. (1997), "Seismic fragility of LRC frames with and without masonry infill walls", *Journal of Earthquake Engineering* 1(4): 693–719.
- Musson, R.M.W. (2005), "Against fractiles", *Earthquake Spectra* 21(3): 887–891.
- National Research Council (1999). The impacts of natural disasters: a framework for loss estimation, National Academy Press, Washington, D.C.
- NEHRP (2011), Selecting and scaling earthquake ground motions for performing response-history-analyses, NIST GCR 11-917-15, prepared by NEHRP Consultants Joint Venture for U.S. Department of Commerce, NIST, Engineering Laboratory Gaithersburg, Maryland.
- Patchett, A., Robinson, D., Dhu, T., Sanabria, A. (2005), Investigating Earthquake Risk Models and Uncertainty in Probabilistic Seismic Risk Analyses, Geoscience Australia Record 2005/02. Canberra, Geoscience Australia: 83.
- Pinto, P.E., Giannini, R. and Franchin, P. (2004), Methods for Seismic Reliability Analysis of Structures, IUSS Press, Pavia, Italy.
- Power, M., Chiou, B., Abrahamson, N., Bozorgnia, Y., Shantz, T., Roblee, C. (2008), "An overview of the NGA project", *Earthquake Spectra* 24(1): 3–21.
- Robinson, D., Fulford, G. Dhu, T. (2006). EQRM : Geoscience Australia's earthquake risk model : technical manual version 3.0. Canberra: Geoscience Australia.
- Rossetto, T, Elnashai, A. (2003). "Derivation of vulnerability functions for European-type RC structures based on observational data", *Engineering Structures* 25(10): 1241–1263.
- Rossetto, T., Elnashai, A. (2005). "A new analytical procedure for the derivation of displacement-based vulnerability curves for populations of RC structures", *Engineering Structures* 7(3): 397–409.
- Rossetto, T., Ioannou, I., Grant, D.N., Mqsood, T. (2014). Guidelines for empirical vulnerability assessment, GEM Technical Report 2014-X, GEM Foundation.
- Rota, M., Penna, A., Magenes, M. (2010), "A methodology for deriving analytical fragility curves for masonry buildings based on stochastic nonlinear analyses", *Engineering Structures* 23:1312-1323.
- Rota, M., Penna, A., Strobbia, C. (2006), "Typological fragility curves from Italian earthquake damage data", First European Conference on Earthquake Engineering and Seismology, Geneva, Switzerland.
- Ruiz-Garcia, J., Miranda, E. (2005), Performance-based assessment of existing structures accounting for residual displacements, The John A. Blume earthquake Engineering Center, Report No. 153, Stanford University.



- Ruiz-Garcia, J., Miranda, E., (2007), "Probabilistic estimation of maximum inelastic displacement demands for performance-based design", *Earthquake Engineering and Structural Dynamics* 36: 1235–1254.
- Ryu, H., Luco, N., Uma, S.R., Liel, A.B. (2011), "Developing fragilities for mainshock-damaged structures through incremental dynamic analysis" Proceedings of the Ninth Pacific Conference on Earthquake Engineering Building an Earthquake-Resilient Society, Auckland, New Zealand.
- Sabetta, F., Pugliese, A. (1996), "Estimation of response spectra and simulation of nonstationary earthquake ground motions", *Bulletin of Seismological Society of America* 86(2): 337–352.
- Sabetta, F., Pugliese, A. (1987), "Attenuation of peak horizontal acceleration and velocity from Italian strong-motion records", *Bulletin of the Seismological Society of America* 77(5): 1491-1513.
- Sabetta, F., Goretti, A., Lucantoni, A. (1998), "Empirical fragility curves from damage surveys and estimated strong ground motion", 11th European Conference on Earthquake Engineering, Balkema, Rotterdam.
- SAC Joint Venture (2000), Recommended seismic evaluation and upgrade criteria for existing welded steel moment-frame buildings, Washington, D.C., prepared for the Federal Emergency Management Agency, FEMA-351.
- SAOC (1995), Vision 2000: Performance Based Seismic Engineering of Buildings, Structural Engineers Association of California, U.C. Berkeley.
- SES 2002. Simulador de Escenarios Sísmicos (SES 2002). Estimación rápida preliminar de daños potenciales en España por terremotos. Manual de usuario. Dcción. Gral. de Prof. Civil. Disponible en: www.proteccioncivil.org/pefn/gt/manuales/m_usuario.pdf SES 2002. Simulador de Escenarios Sísmicos 2002. Dirección General de Protección Civil. CD Rom. DGPC (ed). 2002.
- Shibata, A., Sozen, M. (1976). "Substitute structure method for seismic design in reinforced concrete", *ASCE Journal of Structural Engineering* 102(1): 1–18.
- Shinozuka, M., Feng, M.Q., Kim, H., Kim, S. (2000). "Nonlinear static procedure for fragility curve development", *Journal of Engineering Mechanics* 126: 1287-1295.
- Singhal, A., Kiremidjian, A.S. (1996). "Method for probabilistic evaluation of seismic structural damage", *Journal of Structural Engineering* 122: 1459–1467.
- Spence, R. (2007). Earthquake disaster scenario predictions and loss modelling for urban areas, LESSLOSS Report No., 2007/07, Pavia: IUSS Press.
- Spence, R., Foulser-Piggott, R. (2013), "The use of macroseismic intensity as a basis for empirical vulnerability assessment", Vienna Congress on Recent Advances in Earthquake Engineering and Structural Dynamics 2013, Vienna, Austria, paper no. 374.
- Spence, R., Coburn, A.W., Pomonis, A. (1992). "Correlation of ground motion with building damage: The Definition of a New Damage-Based Seismic Intensity Scale", Proceedings of the Tenth World Conference on Earthquake Engineering, Madrid, Spain, Vol. 1, pp. 551–556.



- Sokolov, V., Wenzel, F., (2011), "Influence of spatial correlation of strong ground motion on uncertainty in earthquake loss estimation", *Earthquake Engineering and Structural Dynamics* 40(9): 993–1009.
- Stafford, P.J., Stasser, F.O., Bommer, J.J. (2007), Preliminary report on the evaluation of existing loss estimation methodologies, Department of Civil & Environmental Engineering, Imperial College London.
- Standards Australia (2007). AS 1170.4-2007: Structural design actions, Part 4: Earthquake actions in Australia. Sydney: Standards Australia.
- Toro, G.R., Abrahamson, N.A., Schneider, J.F. (1997), "Model of Strong Ground Motions from Earthquakes in Central and Eastern North America: Best Estimates and Uncertainties", *Seismological Research Letters* 68(1): 41–57.
- Uma, S.R., Dhakal, R.P., Nayerloo, M. (2014). "Evaluation of displacement-based vulnerability assessment methodology using observed damage data from Christchurch", *Earthquake Engineering and Structural Dynamics*, DOI: 10.1002/eqe.2450.
- Vamvatsikos, D., Cornell, C.A., (2006), "Direct estimation of the seismic demand and capacity of oscillators with multi-linear static pushovers through IDA", *Earthquake Engineering and Structural Dynamics* 35(9): 1097–1117.
- Whitman, R.V., Reed, J.W., Hong, S.T. (1973). "Earthquake damage probability matrices", Proceedings of the Fifth World Conference on Earthquake Engineering, Rome, Italy, Vol. 2, pp. 2531–2540.
- Wills, C.J., Clahan, K.B. (2006), "Developing a map of geologically defined site-condition categories for California", *Bulletin of the Seismological Society of America* 96(4): 1483–1501.
- Wu, Y.M., Hsiao, N.C., Teng, T.L. (2004). "Relationships between strong ground motion peak values and seismic loss during the 1999 Chi-Chi, Taiwan earthquake", *Natural Hazards* 32(3): 357-373.
- Yang, W.S., Slejko, D., Viezzoli, D., Gasparo, F. (1989), "Seismic risk in Friuli-Venezia Giulia: an approach", *Soil Dynamics and Earthquake Engineering* 8(2): 96-105.
- Yong, C., Ling, C., Guendel, F., Kulhanek, O., Juan, L. (2002), "Seismic hazard and loss estimation for Central America", *Natural Hazards* 25(2): 161-175.